International Journal of Scientific Interdisciplinary Research

Volume: 1; **Issue:** 1
Pages: 194–237

MODELLING THE IMPACT OF TEMPERATURE COEFFICIENTS ON PV SYSTEM PERFORMANCE IN HOT AND HUMID CLIMATES

MD Hamidur Rahman[1];

[1]. Bachelor of science in Electrical and Electronic Engineering, American International University-Bangladesh, Dhaka, Bangladesh; Email: hamidurr99@gmail.com

Doi: 10.63125/abj6wy92

Received: *21 September 2022;* ***Revised:*** *27 October 2022;* ***Accepted:*** *29 November 2022;* ***Published:*** *24 December 2022;*

Abstract

This quantitative study examined how temperature coefficients shaped photovoltaic (PV) system performance in hot and humid climates through 12-month, minute-resolution monitoring and coefficient-aware modeling across three representative installations: a coastal roof-flush site, an urban roof-standoff site, and an inland rack-mounted site, including crystalline-silicon and thin-film technologies. Descriptive findings indicated persistent thermal stress, with plane-of-array irradiance averaging 715–768 W/m², ambient temperatures averaging 30.4–33.2°C, and module temperatures averaging 44.8–49.6°C. Relative humidity remained high (73.6–81.9%) and wind speeds were modest (1.6–2.4 m/s), producing sustained module heating above ambient. Under these conditions, normalized DC power averaged 0.84–0.89 p.u., confirming baseline thermal derating during productive hours. Correlation results showed that module temperature was strongly and negatively associated with voltage and power outputs, including open-circuit voltage (r = −0.71), normalized DC power (r = −0.62), and efficiency (r = −0.63), while associations with short-circuit current were weakly positive or near zero (r = 0.06), supporting voltage-dominated thermal losses. Site-level multivariate regressions controlling for irradiance, wind, humidity, and ambient temperature confirmed an independent temperature penalty on normalized DC power, with coefficients of −0.0043, −0.0037, and −0.0030 p.u./°C (all p < .001) and strong model fits (adjusted R^2 = 0.84–0.88; RMSE = 0.058–0.069 p.u.). Mixed-effects pooling showed crystalline silicon to be more temperature-sensitive than thin-film, consistent with more negative effective power slopes in silicon arrays. Using field-effective coefficients reduced prediction error compared with datasheet coefficients (RMSE 0.064 vs 0.091) and lowered annual yield estimates by about 4.7%. Overall, the results demonstrated that climate-calibrated temperature coefficients and accurate module-temperature modeling were essential for realistic PV yield prediction in hot and humid environments.

Keywords

Temperature Coefficients, PV Performance, Hot-Humid Climates, Thermal Derating, Energy Yield.

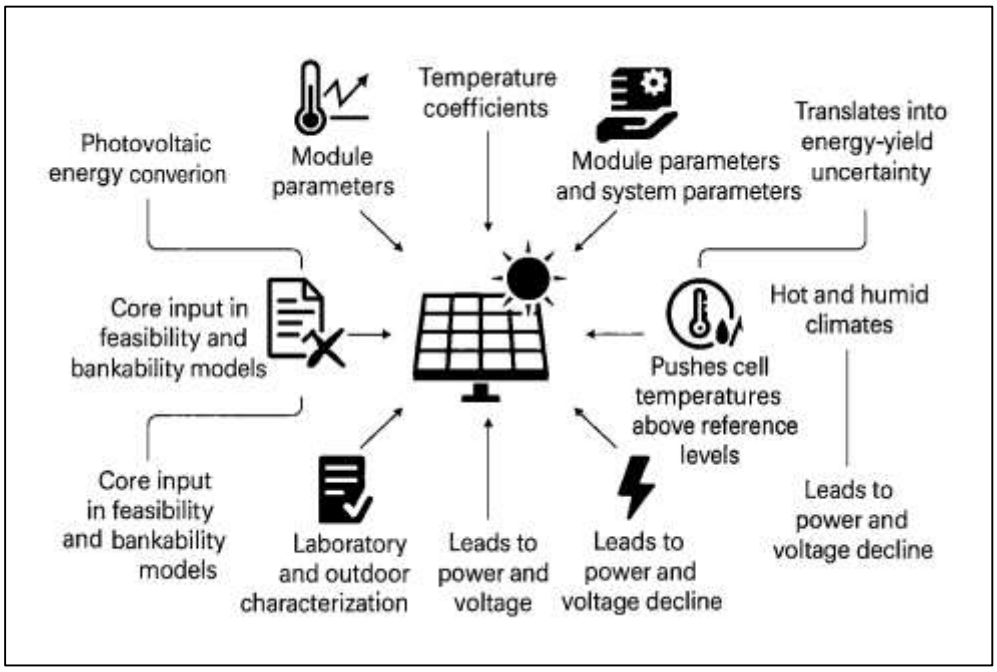
INTRODUCTION

Photovoltaic energy conversion is the process of generating electrical power directly from sunlight using semiconducting materials that exhibit the photovoltaic effect (Sivula & Van De Krol, 2016). A PV system is typically defined as an arrangement of one or more solar modules, power-conditioning equipment, and balance-of-system components that together convert solar irradiance into usable electricity at the load or grid interface. In quantitative performance analysis, PV output is modeled as an environmental–electrical transformation in which irradiance provides the driving input while module and system parameters regulate conversion efficiency. One of the most influential parameters is the temperature coefficient, which denotes the rate of change of a PV electrical variable per unit change in cell or module temperature relative to a reference condition. Temperature coefficients are commonly specified for maximum power, open-circuit voltage, short-circuit current, and sometimes fill factor, and they express how sensitive these outputs are to heat. International PV practice emphasizes temperature coefficients because nearly all operating environments deviate from standard rating temperatures, and the resulting deviations translate into energy-yield uncertainty, financial risk, and planning error. Hot and humid climates carry particular global importance: they include densely populated tropical and subtropical regions where electricity demand is rising, solar resources are strong, and PV deployment has become a cornerstone of decarbonization and energy-access strategies (Sampaio & González, 2017). In these regions, ambient temperatures remain high for extended periods, humidity alters heat dissipation pathways, and the combined effect pushes cell temperatures well above reference levels. Multiple field investigations from equatorial Asia, coastal Africa, and tropical island systems have reported that modules frequently operate far above nominal temperatures during peak irradiance, producing measurable power derating. Laboratory and outdoor characterization studies across crystalline silicon and thin-film technologies have repeatedly shown that power and voltage decline as temperature rises, while current may increase slightly, leading to a net negative power response for most commercial modules. Energy planners and financiers therefore treat temperature coefficients as core inputs in feasibility models, performance guarantees, and bankability assessments (Bayod-Rújula, 2019). A quantitative paper on modeling temperature-coefficient impacts in hot and humid climates begins with these definitions because they anchor the conceptual relationship between thermal stress and electrical output. The task is not merely descriptive: it requires formalizing how coefficients interact with local meteorology, module physics, and system design so that predicted energy production aligns with real operation in these internationally significant environments.

Performance modeling of PV systems has evolved through a long sequence of empirical, semi-empirical, and physics-based approaches, each placing temperature and its coefficients at the center of output estimation. Early correction models extended standard ratings to field conditions by applying linear derating factors derived from temperature coefficients and estimated module temperatures. These methods became attractive for their simplicity and were widely adopted in engineering practice (Green & Bremner, 2017). Later work introduced heat-balance formulations that compute module temperature from absorbed irradiance, convective exchange with surrounding air, radiative losses to the sky, and conduction to mounting structures. Such formulations form the backbone of many widely used simulation packages and research models. Comparative studies across commercial tools have shown that temperature treatments, and therefore coefficient applications, can be a primary source of divergence in predicted yields between models. A consistent finding from many datasets is that voltage-related variables show stronger temperature sensitivity than current-related variables, meaning that even small errors in estimating module temperature propagate into notable power-prediction bias. Researchers have explored the dependence of coefficients on irradiance and operating point, observing that coefficients measured under controlled laboratory temperatures may not reproduce outdoor behavior when irradiance levels or spectral composition shift. Multi-site validation campaigns in warm regions have highlighted that model accuracy improves when coefficients are calibrated for the specific technology and climate rather than taken as universal constants (Haque et al., 2018). Technology comparisons involving monocrystalline and multicrystalline silicon, CdTe, CIGS, and amorphous silicon have demonstrated distinct coefficient magnitudes, reflecting differences in band gap, recombination pathways, and resistive losses. Several studies focusing on tropical rooftops

and utility-scale arrays have shown that modules with smaller-magnitude negative power coefficients can outperform others under sustained heat, although that advantage depends on site-specific temperature regimes and airflow. This body of research motivates coefficient-focused modeling as a quantitative challenge: the coefficient is not only a datasheet number but a statistical parameter whose effective value can vary with environment, technology, and system configuration. Modeling in hot and humid climates therefore requires a clear explanation of coefficient use within the broader modeling tradition, including how temperature is estimated, how coefficients enter electrical equations, and how uncertainties in either component affect predicted performance (Pushpakaran et al., 2016).

Figure 1: Photovoltaic Temperature Coefficients: Humid Climates



Hot and humid climates shape PV thermal behavior through interacting atmospheric mechanisms that differ from those in dry or temperate regions. In many tropical locations, high ambient temperatures persist across diurnal cycles, raising the baseline around which module temperatures fluctuate. Humidity modifies air density, moisture content, and boundary-layer characteristics near the module surface, which in turn affects convective cooling rates (Arfan et al., 2021; Rawat et al., 2017). Frequent cloud formation and rapid cloud passage typical of tropical meteorology introduce strong short-term irradiance variability that can heat and cool modules in pulses, while the module's thermal mass creates lagged temperature response (Ferdous Ara, 2021). Field observations in coastal and equatorial zones show that module temperature can remain elevated even when irradiance drops, producing moments of coefficient-driven derating under partially diffuse light (Jahid, 2021; Akbar & Farzana, 2021). Studies of mounting geometry report that roof-mounted arrays in dense tropical cities often run hotter than elevated rack systems because reduced air circulation increases the thermal resistance between module and ambient air (Reza et al., 2021; Saikat, 2021). In humid regions with low wind speeds, this effect intensifies, especially during midday hours when irradiance is highest and air stagnation is common. The tropical sky also influences long-wave radiation exchange; high water vapor content and cloud layers reduce night-sky cooling, limiting overnight temperature recovery (Shaikh & Aditya, 2021; Kanti & Shaikat, 2021; Xiang et al., 2019). Research conducted at multiple tropical test sites has consistently measured cell temperatures exceeding ambient by several tens of degrees Celsius, with the exact gap governed by wind, tilt, surface emissivity, and rear-side ventilation (Zobayer, 2021a, 2021b). These elevated temperatures activate negative power coefficients continuously through much of the year, which can lower annual energy yield compared with estimates that assume temperate operating conditions. Humidity is also associated with precipitation cycles and aerosol behavior, affecting soiling and surface wetting. These factors change the absorbed fraction of irradiance and can either increase

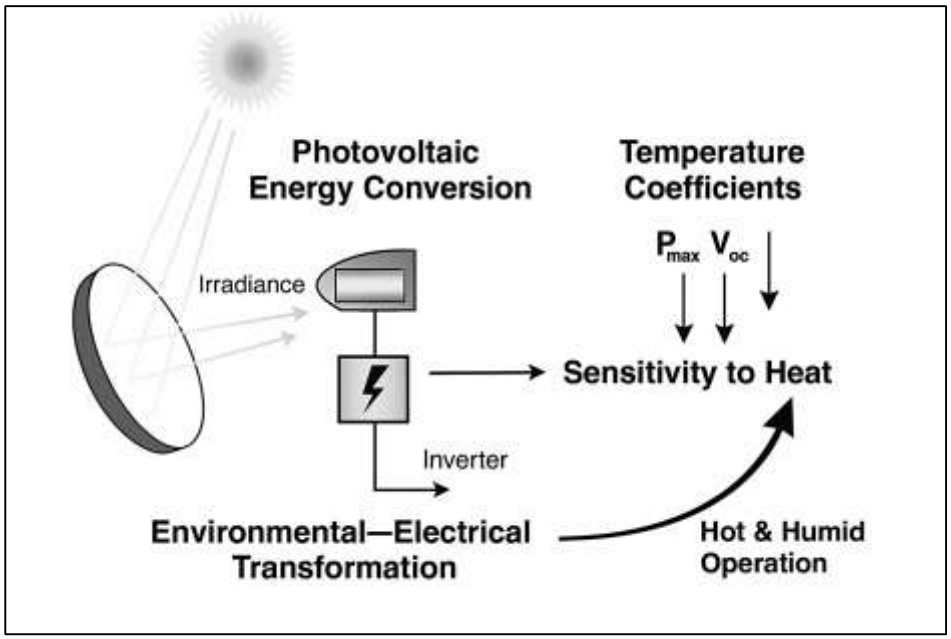
heating through higher absorption or reduce heating when cloudiness dominates, complicating statistical separation of thermal and optical influences (Ariful & Ara, 2022; Arman & Kamrul, 2022). For quantitative modeling, the key point is that temperature in hot and humid climates is both higher in mean value and more tightly coupled to meteorological co-variables, so coefficient impacts cannot be isolated using simplistic assumptions (Mesbaul & Farabe, 2022; Nahid, 2022). An extended introduction must therefore articulate how tropical heat, moisture, wind, and irradiance dynamics interact to shape module temperature trajectories and thus the realized influence of temperature coefficients on performance (Sánchez et al., 2019; Hossain & Milon, 2022; Abdur & Haider, 2022).

At the device-physics level, temperature coefficients arise from fundamental semiconductor responses to heat and provide a mechanistic explanation for field-observed derating (Mushfequr & Praveen, 2022; Mortuza & Rauf, 2022). In crystalline silicon, elevated temperature narrows the band gap, increasing intrinsic carrier concentration and enhancing recombination, which reduces open-circuit voltage in an approximately linear manner across normal operating ranges. The reverse saturation current in the diode representation rises steeply with temperature, reinforcing voltage loss under load (Kaushika et al., 2018; Rakibul & Samia, 2022; Rony & Ashraful, 2022). Short-circuit current often increases slightly with temperature because of improved carrier generation, but this gain is small relative to voltage decline, leading to net power reduction. Fill factor also tends to decrease as temperature elevates resistive and recombination losses, further contributing to negative power coefficients. Thin-film modules exhibit different balances (Saikat, 2022; Shaikh & Sudipto, 2022): their wider band gaps or distinct recombination pathways can make voltage less temperature-sensitive, producing smaller negative power coefficients, although the direction and magnitude depend on technology variant and manufacturing details . Numerous characterization experiments have extracted temperature coefficients using stabilized temperature sweeps while holding irradiance constant, and they consistently reveal that the slope for voltage dominates the slope for power (Huen & Daoud, 2017). Outdoor I–V tracing campaigns add a second layer of evidence by showing that coefficients can shift with irradiance level, because series resistance and shunt pathways change their relative importance at different currents. In hot and humid climates, the co-variation between high irradiance and high temperature amplifies these nonlinearities, sometimes yielding effective coefficients that differ from laboratory values. Long-duration tropical monitoring studies also report that thermal and moisture stress can alter encapsulant properties, contact resistances, and interconnect integrity, gradually shifting the electrical parameters that underlie coefficient values. Moisture ingress, corrosion, and polymer aging contribute to evolving resistive terms that can change how voltage responds to temperature over time. For quantitative modeling, these findings imply that coefficients should be treated as parameters grounded in physics but sensitive to operating context (Brusso, 2019). A robust introduction should lay out these physical pathways to justify why coefficient-based performance prediction is credible, why most coefficients are negative for power, and why effective coefficients in hot, humid operation may require site-specific calibration even when the underlying semiconductor theory remains the same.

When moving from module behavior to full PV systems, temperature coefficients shape not only instantaneous power but also array mismatch, control performance, and annual energy yield (Guney, 2016). System-level temperature depends on spatial layout, row spacing, tilt, surface reflectance, and the thermal characteristics of mounting structures. Studies analyzing array temperature maps in warm climates show that edge modules cool more effectively than interior modules, and airflow corridors between rows create systematic temperature gradients. These gradients translate into voltage differences between strings and can increase mismatch losses, which are magnified when negative power coefficients depress hotter modules more strongly. MPPT algorithms track the maximum power point as it shifts with temperature; higher temperatures move the operating voltage downward, so controller efficiency and voltage window constraints determine how fully the system can exploit available current (Bierman et al., 2016). In hot climates, the MPP can approach inverter low-voltage limits during peak heat, particularly for strings designed near nominal temperatures, yielding additional losses that are inherently tied to coefficients. Rapid irradiance swings in humid tropical weather also affect the interaction between thermal inertia and electrical tracking. Modules cool and

heat more slowly than irradiance changes, so transient states occur where irradiance is high enough to drive power but temperatures remain elevated from a prior sunny interval, producing short-term coefficient losses that may be missed in hourly simulations (Khaligh & Onar, 2017). Several high-resolution monitoring studies in tropical regions have demonstrated that sub-hourly models better capture these lags and improve energy-yield agreement with measurements. Degradation behavior in hot and humid locations further couples to coefficients because elevated operating temperatures accelerate chemical and mechanical aging. As modules degrade, series resistance and recombination behavior shift, which can modify measured coefficients and alter future output response to temperature. For plant developers and grid operators working in tropical economies, these system-level interactions affect capacity-factor estimates, reserve margins, and the achievable penetration of PV. The quantitative focus on temperature coefficients is therefore not narrow; it is a systems question about how thermal sensitivity propagates through real-world layouts, electronics, and operational variability (Zhang et al., 2019). An extended introductory framing should connect coefficients to these array and plant behaviors so the reader sees why accurate coefficient modeling matters for system performance assessment in hot and humid climates.

Figure 2: Temperature Coefficients in Humid PV



Reliable coefficient-aware modeling depends on measurement and parameterization strategies that are valid under humid and high-temperature conditions. Standard coefficient extraction relies on controlled tests where modules are stabilized at multiple temperatures and their I–V curves measured under fixed irradiance to derive linear slopes (Behura et al., 2019). Field-based approaches instead infer coefficients by regressing measured power or voltage against estimated cell temperature over long periods. In tropical environments, these strategies face added complexities. Back-sheet sensors and thermocouples must be moisture-protected and properly bonded, because humidity and surface wetting can change sensor thermal contact and response time. Site studies comparing sensor locations show that small placement differences can bias inferred coefficients, especially when rear-side ventilation varies or when rain events temporarily cool surfaces unevenly. Infrared thermography has been used to map temperature heterogeneity across modules in humid climates, identifying hot spots from partial shading, soiling patterns, or moisture-related defects that influence coefficient estimation. Many outdoor calibration campaigns report that effective coefficients derived from real operation can diverge from manufacturer values, with divergence linked to irradiance distribution, local wind regime, and mounting configuration (Guney, 2016). Researchers have responded by combining physically based temperature models with statistical estimation, jointly calibrating temperature parameters and coefficients to reduce identifiability problems that arise from correlated meteorological

drivers. Multi-year tropical datasets have also motivated the use of robust regression and filtering to remove periods influenced by rain cooling, transient shadows, or sensor anomalies. These methodological advances underscore a central quantitative issue: uncertainty in module temperature estimation is often the largest contributor to uncertainty in coefficient-adjusted yield prediction. Therefore, coefficient modeling in hot and humid climates cannot be separated from how temperature is measured and modeled (Bierman et al., 2016). An introduction should highlight why humid tropical measurement conditions require careful data handling, why effective coefficients are context-sensitive, and why the quantitative modeling task must integrate thermal modeling and coefficient estimation rather than treating either as an isolated step.

Statistical and computational frameworks provide the final conceptual pillar for modeling the impact of temperature coefficients in hot and humid climates (Khaligh & Onar, 2017). Linear models remain the baseline for expressing power loss per degree of temperature increase, and they are widely used for quick derating estimates and performance guarantees. However, extensive research on tropical PV performance shows that linearity is often an approximation over limited temperature and irradiance bands, because irradiance–temperature coupling can induce curvature in the power–temperature relationship. Multivariate regression frameworks incorporate irradiance, wind speed, humidity proxies, and sometimes sky temperature to improve coefficient attribution. Mixed-effects models have been applied to multi-site tropical datasets to separate technology-specific fixed effects from site-specific random effects, clarifying how coefficients vary across coastal, inland, and high-altitude humid zones. Physics-informed simulations based on the single-diode equation coupled with heat-balance temperature models allow scenario-based quantification of coefficient sensitivity to mounting height, ventilation, albedo, and module technology (Zhang et al., 2019). Data-driven forecasting studies using machine-learning regressors frequently identify temperature and temperature-derived features as dominant predictors of power variation during hot spells, supporting the empirical importance of coefficients even within flexible nonlinear models. Cross-validation work comparing hourly and sub-hourly simulation indicates that higher temporal resolution can better represent thermal lags common in tropical cloud regimes, improving the modeled coefficient impact on short-term and annual yield. Regional scaling studies combining meteorological reanalysis with site monitoring have constructed coefficient-aware yield maps for tropical countries, illustrating large geographic gradients in expected thermal derating. Across these approaches, a recurring quantitative finding is that treating coefficients as fixed universal constants leads to systematic yield bias in hot and humid climates, while locally calibrated or dynamically adjusted coefficients reduce error. An extended introduction should synthesize these modeling options, not to claim finality, but to show the methodological landscape in which coefficient-focused quantitative analysis resides (Behura et al., 2019). By aligning definitions, climate mechanisms, device physics, system interactions, measurement practices, and statistical tools, the introductory foundation prepares for a rigorous quantitative examination of how temperature coefficients regulate PV system performance under sustained heat and moisture.

The primary objective of this quantitative study is to model and measure how temperature coefficients govern photovoltaic system performance in hot and humid climates, where operating conditions routinely depart from standard rating environments. Specifically, the study aims to (a) quantify the relationship between module operating temperature and key electrical outputs—maximum power, open-circuit voltage, short-circuit current, and efficiency—using temperature-coefficient formulations that translate thermal variation into electrical derating; (b) estimate effective, field-based temperature coefficients for dominant PV technologies under sustained tropical heat and moisture, and compare these values with nominal datasheet coefficients to determine the extent of climate-driven coefficient drift; (c) integrate a heat-balance temperature sub-model with an electrical performance sub-model to capture how ambient temperature, irradiance intensity, wind regime, and humidity-related convective constraints jointly shape cell temperature trajectories over time; and (d) validate the modeled outputs against high-resolution operational data from PV installations located in representative hot and humid sites, evaluating prediction accuracy at sub-hourly, daily, and annual scales. A further objective is to conduct sensitivity and uncertainty analyses to identify which temperature-coefficient parameters and thermal pathways contribute most to yield-prediction error, thereby isolating the dominant

mechanisms through which tropical environments suppress real-world PV output. The study also seeks to determine how system configuration variables common in humid regions—such as roof-mount proximity, limited rear ventilation, low tilt angles, and frequent cloud-induced irradiance transients—interact with negative power coefficients to amplify mismatch losses and energy shortfalls at the array level. By achieving these objectives, the research will produce a climate-specific, technology-aware modeling framework that represents temperature-coefficient impacts as measurable, calibratable parameters rather than fixed constants, enabling more accurate estimation of performance ratios, capacity factors, and long-term energy yield for PV systems operating under persistent heat and moisture.

LITERATURE REVIEW

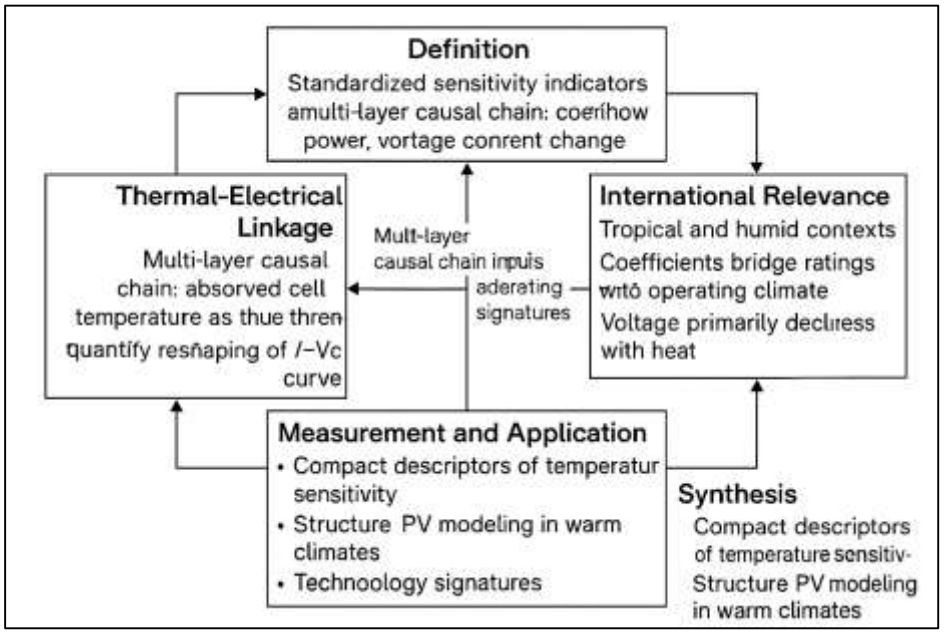
The literature review for this quantitative study synthesizes prior theoretical, empirical, and modeling research on how temperature coefficients shape photovoltaic (PV) system performance, with a focused lens on hot and humid climates. Because PV modules are rated under standardized conditions, the transfer of nameplate specifications to real tropical operating environments requires careful examination of temperature-driven electrical losses (Dupré et al., 2017). Existing scholarship spans semiconductor-level explanations of temperature sensitivity, laboratory extraction of temperature coefficients, outdoor validation of coefficient effectiveness, and system-scale simulations that incorporate thermal sub-models. However, the evidence base is distributed across technologies, climates, and modeling assumptions, creating a need for a structured synthesis that explicitly links temperature coefficients to yield prediction accuracy in humid heat regimes (Cuce et al., 2017). Accordingly, this review critically maps how module temperature is modeled in the presence of irradiance, wind, and humidity interactions; how coefficients vary across PV technologies and measurement settings; and how these coefficients propagate through array mismatch, inverter operating limits, and annual energy yield estimates. By organizing and evaluating these strands, the review establishes the quantitative grounding for the study's modeling framework, clarifies what is already known about coefficient behavior in tropical conditions, and identifies methodological gaps in coefficient calibration, uncertainty treatment, and climate-specific validation that the present research addresses (Toledo et al., 2020).

Temperature Coefficients in PV Performance

Temperature coefficients occupy a foundational role in photovoltaic (PV) performance analysis because they formalize how PV electrical behavior responds to heat under real operating conditions (Tabor et al., 2018). Across the PV literature, temperature coefficients are consistently defined as standardized sensitivity indicators: they express how a module's maximum power, open-circuit voltage, short-circuit current, and overall conversion efficiency change per unit increase in cell or module temperature from a reference condition. Studies spanning crystalline silicon and thin-film technologies treat the power temperature coefficient as the most direct summary of thermal loss because it integrates the combined temperature responses of voltage, current, and fill factor into a single measurable slope. Voltage and current coefficients are treated as component sensitivities that explain why power changes in the direction and magnitude observed in field operation, while efficiency coefficients translate temperature effects into system-level conversion terms that correlate with annual yield. Research comparing manufacturer datasheets, laboratory extractions, and outdoor monitoring emphasizes that the reference basis used for coefficients matters: most modules are rated under a standardized reference state designed for comparability rather than realism, and therefore temperature coefficients are meant to bridge the gap between rated and operating conditions (Feron & Monti, 2018). A major theme in the literature is that coefficients are not merely descriptive labels but quantitative parameters that structure modeling, quality assurance, and financial evaluation. They appear in derating models, performance ratios, and energy yield simulations as routine inputs, and they are treated as technology signatures because different materials and device designs yield systematically different sensitivities to temperature. A further conceptual point established in many comparative studies is that coefficients are typically negative for power and voltage in commercial modules, reflecting a universal direction of thermal penalty even if magnitudes differ. In hot-climate performance studies, coefficients are frequently discussed alongside thermal risk, bankability, and system planning because they determine the scale of expected loss in warm environments (S. Li et al., 2020). At this definitional level, the

literature converges on a shared understanding: temperature coefficients provide the primary quantitative link that allows PV output models to move from standardized ratings to climate-specific performance, and they do so by summarizing how thermal stress alters the electrical working point of PV modules in measurable, technology-dependent ways.

Figure 3: Temperature Coefficients Framework for PV



The thermal–electrical linkage behind temperature coefficients is treated in prior research as a multi-layer causal chain that begins with absorbed solar energy and ends with altered electrical output. The literature separates ambient temperature from cell or module temperature, noting that ambient conditions only set the boundary around a module's operating state (Carlucci et al., 2018). Field measurements across climates repeatedly show that cell temperature systematically exceeds ambient temperature because sunlight heats the module, and the module dissipates that heat through convection and radiation at rates governed by wind, mounting geometry, and surface properties. In modeling studies, cell temperature is therefore treated as the thermal variable that directly controls electrical response, while ambient temperature is treated as an indirect driver that shapes cell temperature but cannot substitute for it without substantial error. Across device-level and system-level analyses, researchers demonstrate that voltage responds more strongly to temperature than current, so thermal penalties are dominated by voltage decline. This dominance is explained by semiconductor physics as well as by equivalent-circuit interpretations: as temperature rises, the voltage portion of the current–voltage curve shifts downward because recombination and intrinsic carrier effects increase, and resistive losses intensify, thereby reducing open-circuit voltage and moving the maximum power point to lower voltages (Chen, Vinco, Baek, et al., 2020). Current, in contrast, changes modestly and often upward with temperature because carrier generation improves slightly, yet this increase is too small to offset voltage loss. Multiple outdoor monitoring and laboratory tracing studies show that power loss with temperature closely tracks voltage loss, confirming the quantitative primacy of the voltage coefficient in shaping the power coefficient. A consistent conclusion across different technologies is that fill factor also degrades with heat, reinforcing power decline beyond what voltage alone predicts. These findings have led to performance models that prioritize accurate estimation of cell temperature and robust characterization of voltage sensitivity, especially in locations where temperature and irradiance rise together. Additionally, the literature highlights that the thermal–electrical relationship is not perfectly static: coefficients can vary with irradiance level and operating regime, indicating that temperature sensitivity is best interpreted as an effective parameter that summarizes behavior across realistic conditions rather than as an immutable constant (Chen, Vinco, Pagliari, et al., 2020). Taken together, prior studies establish a coherent thermal–electrical narrative:

environmental heating elevates cell temperature above ambient; the elevated cell temperature reshapes the electrical curve primarily through voltage reduction and fill-factor weakening, and temperature coefficients quantify this reshaping in a way that enables systematic modeling and comparison.

International relevance is major reason temperature coefficients are emphasized so strongly in PV research, and the literature situates coefficient modeling as a global planning necessity rather than a niche technical detail. PV deployment has expanded rapidly in tropical and subtropical regions where solar resources are high and electrification needs are large, and studies covering South and Southeast Asia, equatorial Africa, humid coastal Latin America, and island grids consistently show that warm conditions produce meaningful deviations from standardized performance expectations (Goldsworthy, 2017). In these environments, modules operate at high temperatures for long daily durations, and the negative power coefficient translates into persistent energy losses that accumulate to large annual impacts. International yield assessments and cross-country performance comparisons therefore depend on coefficient-based corrections to avoid systematic overestimation of output in warm climates. The literature shows that this matters for several global stakeholders: utilities require accurate predictions to manage capacity factors and reserve margins; policymakers require reliable estimates to meet renewable targets and justify subsidy structures; and financiers require bankable yield projections to price risk and determine project viability. Many multi-site studies demonstrate that simulations relying solely on standardized test ratings misrepresent real outcomes in hot climates, while simulations incorporating temperature coefficients aligned with local operating temperatures produce forecasts closer to measured yields (Ambaum, 2020). The global emphasis on comparability through standardized reference testing is also discussed as a partial limitation: standard tests allow modules to be compared under identical conditions, but they are not meant to reproduce tropical reality. Temperature coefficients are the standardized mechanism that compensates for this gap by transporting the rating into the operating climate. In the international context, coefficient magnitudes also inform technology selection, as comparative studies show that material systems with smaller negative power coefficients can preserve more yield in persistent heat. Such findings are particularly important where land is scarce and high energy density is needed, because they affect cost per kilowatt-hour and the economics of rooftop or utility-scale expansion (Debnath et al., 2020). Overall, the international literature shares a common position: temperature coefficients are essential for credible global PV forecasting because they allow standardized module ratings to be reconciled with climate diversity, especially the hot and humid regimes that now represent a growing share of global solar capacity and demand.

A final synthesis emerging from the conceptual literature is that temperature coefficients function as both physical descriptors and modeling levers that structure quantitative PV analysis in warm climates. Research on coefficient measurement, interpretation, and application shows that coefficients provide a compact way of embedding device physics into large-scale energy models without requiring full semiconductor re-derivation at every step (Taniguchi, 2020). This compactness explains why coefficients appear across scales: at the module level, they summarize temperature sensitivity of power, voltage, current, and efficiency; at the array level, they explain mismatch patterns created by temperature gradients; and at the plant level, they enable thermal derating within energy-yield simulations and performance ratio benchmarking. Numerous studies highlight those coefficients derived in laboratories may differ from those inferred outdoors, because real operation involves co-varying irradiance, wind, humidity, and transient weather dynamics. This has led to the widespread use of "effective" coefficients in performance studies, meaning coefficients estimated from long-term field data that reflect the actual thermal–electrical pathway under local conditions. In hot and humid contexts, field-effective coefficients often become especially important because humidity alters convective cooling and cloud patterns create rapid irradiance changes that interact with thermal inertia (Cleri, 2016). The literature repeatedly shows that inaccurate temperature coefficients propagate directly into yield error: if the coefficient magnitude is underestimated, modeled output remains too optimistic during high-temperature periods; if it is overestimated, models suppress output excessively during cooler intervals. These sensitivities motivate careful coefficient handling in quantitative work, including the separation of ambient and cell temperature, the consideration of mounting-driven

temperature differences, and the accounting for technology-specific coefficient ranges. Another theme in prior studies is that coefficients may drift with aging under thermal and moisture stress, as material degradation alters resistive and recombination behaviors that underlie temperature response. As a result, some long-duration monitoring research treats coefficients as parameters that can be recalibrated over time to sustain model accuracy in humid heat. Conceptually, this positions temperature coefficients not as static datasheet annotations but as empirically grounded variables that require climate awareness and, where possible, local validation (West et al., 2016). When these strands are combined, the literature provides a clear conceptual platform for quantitative modeling in hot and humid climates: temperature coefficients define the measurable sensitivity of PV outputs to operating heat, voltage response dominates the loss mechanism, cell temperature is the true control variable distinct from ambient temperature, and global PV expansion in warm regions makes coefficient-accurate modeling indispensable for credible performance prediction.

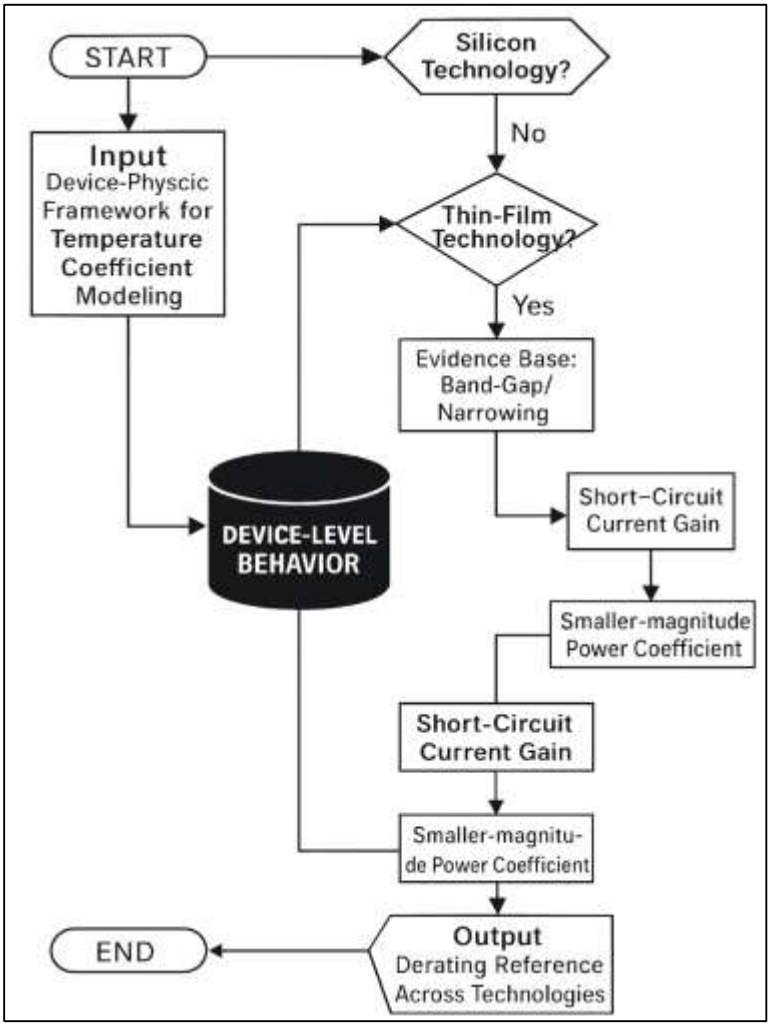
Device-Level Physics Behind Temperature Sensitivity (Quantitative Emphasis)

Device-level temperature sensitivity in silicon photovoltaic technologies has been examined extensively because crystalline silicon remains the dominant commercial platform and exhibits a well-characterized decline in electrical output as temperature rises (Moser et al., 2016). Across experimental and modeling studies, the central physical driver is band gap narrowing in silicon at elevated temperatures, which reduces the energy separation required for carrier excitation and shifts the current–voltage profile primarily through voltage depression. This manifests most clearly as a decline in open-circuit voltage, a variable repeatedly shown to be more thermally sensitive than short-circuit current in silicon devices. The physics literature explains that voltage loss is amplified by the exponential growth of saturation current with temperature, linked to higher intrinsic carrier concentration and intensified recombination. These coupled effects steepen the voltage drop under load and shift the maximum power point to lower operating voltages. Although short-circuit current tends to rise mildly with temperature due to slightly improved carrier generation, the magnitude of that gain is consistently reported as small compared with voltage reductions, so the net result is a negative power response (Ye et al., 2019). Quantitative characterizations of commercial mono- and multicrystalline silicon modules regularly show that power temperature coefficients are moderately negative and clustered within relatively narrow bands across manufacturers, reinforcing the idea that silicon temperature sensitivity is both predictable and materially constrained by semiconductor properties. Laboratory temperature sweeps and outdoor current–voltage tracing campaigns align on this direction of change, while also documenting that the relative contributions of voltage decline and fill-factor weakening vary by cell architecture, metallization, and encapsulation. The literature also notes that series resistance and shunt pathways are indirectly temperature affected, so silicon modules with higher resistive losses at baseline tend to show stronger power loss rates as temperature rises. In hot, humid environments where operating temperatures remain elevated for long durations, these device-level behaviors scale into persistent derating that can dominate annual yield differences among otherwise similar silicon systems (Steinkemper et al., 2017). Overall, the silicon-focused evidence base establishes a coherent causal profile: thermal elevation reduces voltage substantially through band gap and saturation-current mechanisms, current increases only marginally, and the resulting power sensitivity is negative and measurably stable across silicon product classes, providing a consistent physical foundation for coefficient-based modeling.

Thin-film photovoltaic technologies display temperature sensitivity patterns that differ in magnitude and sometimes in the balance of contributing electrical variables because their semiconductor compositions and recombination pathways contrast with silicon. Comparative device studies on cadmium telluride, copper indium gallium selenide, and amorphous silicon highlight that wider or differently structured band gaps can reduce the extent of voltage degradation per degree of temperature increase, which is why thin-film power temperature coefficients are often reported as less negative than those of crystalline silicon (M. Li et al., 2020). In cadmium telluride modules, field and laboratory investigations commonly find relatively restrained voltage sensitivity, attributed to material-specific band-gap behavior and recombination kinetics that respond differently to heat. Copper indium gallium selenide devices show a similarly moderated voltage decline in many datasets, though the spread of reported coefficients is larger, reflecting broader manufacturing diversity and

sensitivity to absorber quality and buffer-layer interfaces. Amorphous silicon adds further complexity because its temperature response interplays with light-induced defect dynamics and partial thermal annealing, producing temperature coefficients that may change slightly with exposure history and operating regime. These physical distinctions translate into technology-specific coefficient distributions evident in multi-technology field trials conducted in warm regions: thin films frequently retain a larger fraction of rated power under the same cell temperature compared with silicon, yet their absolute energy yield advantage depends on local irradiance patterns, spectral content, and degradation behavior (Surya et al., 2019).

Figure 4: Device-Level PV Temperature Sensitivity Framework



The literature documents that thin-film modules may heat to similar absolute temperatures as silicon under equal mounting conditions, meaning that their relative benefit in hot climates comes from smaller thermal sensitivity rather than cooler operation. Studies that disaggregate power sensitivity into voltage and current components show that thin films often experience smaller voltage penalties and comparable or slightly larger current increases with temperature, reinforcing their reduced net power loss. At the same time, device research cautions that encapsulant moisture interactions and contact stability vary across thin films, so coefficient magnitude is only one dimension of hot–humid suitability. Taken as a whole, thin-film temperature-sensitivity scholarship provides a contrasting physical template to silicon: material band-gap and recombination traits soften voltage loss, yielding smaller-magnitude negative power coefficients in many cases, while technology-specific spreads underline the importance of distinguishing among thin-film families rather than treating them as a uniform class (Giner et al., 2018).

Across both silicon and thin-film technologies, the literature shows that temperature coefficients are

not invariably constant across operating conditions, and nonlinearities become especially visible at high irradiance and high temperature combinations typical of hot climates. Many controlled studies report that coefficients extracted under moderate irradiance can shift when irradiance rises, because internal resistive losses, carrier-collection efficiency, and recombination balance change with operating current (Ma et al., 2018). This irradiance dependence appears in outdoor measurements where temperature and irradiance co-vary, producing effective coefficients that differ from laboratory baselines, even when the direction of temperature response remains stable. A closely related mechanism is fill-factor degradation under heat. Device-level analyses using current–voltage curve decomposition show that as temperature increases, the curve becomes less "square" due to rising saturation current and resistive effects, lowering fill factor and magnifying power loss beyond what voltage decline alone would imply. This contribution is quantitatively important in modules with higher series resistance or weaker shunt integrity, and it helps explain why two modules with similar voltage coefficients can still display different power coefficients (Sangwan & Hersam, 2020). The modeling literature further notes that the choice between one-diode and two-diode electrical representations affects the implied temperature dependence because the two-diode model separates recombination channels that respond differently to heat. When two-diode parameters are estimated from temperature-swept data, the resulting power sensitivity can reflect more complex curvature, particularly at low to moderate irradiance where recombination in the depletion region matters more. In contrast, one-diode models often compress these effects into a single saturation-current term, yielding smoother linear approximations. Empirical comparisons across devices indicate that nonlinear temperature sensitivity is more pronounced in modules operating near high-current regions, such as midday tropical conditions, when resistive heating and carrier-density effects peak (Rezaei et al., 2020). The cumulative evidence frames nonlinearities as systematic rather than random: they arise from physical processes that scale with irradiance and temperature simultaneously, and they appear consistently across measurement platforms. This is why a sizable portion of device-focused PV scholarship treats coefficients as effective parameters conditioned by the operational envelope, highlighting that coefficient-based modeling in hot climates benefits from calibration using data that cover the high-irradiance, high-temperature regime rather than relying only on mild-condition extractions.

Device-level physics studies also emphasize that technology comparisons of temperature sensitivity must be interpreted through the joint lens of semiconductor response and parameter extraction context. Large experimental datasets indicate that while silicon and thin films show distinct average coefficient magnitudes, the spread within each category is meaningful and linked to cell architecture, contact design, and material quality (Pazos et al., 2020). For silicon, passivated emitter rear contact structures, heterojunction designs, and back-contact cells show slightly different temperature sensitivities compared with conventional architectures, reflecting variations in recombination suppression and resistive pathways. For thin films, absorber stoichiometry, grain structure, and interface engineering help explain why coefficient distributions for cadmium telluride and CIGS are broader than those for crystalline silicon. The literature also underscores that coefficient estimation itself can introduce apparent differences, because coefficients derived from stabilized laboratory steps are not identical to those inferred from outdoor regression when irradiance fluctuates and thermal inertia creates lags. Device papers comparing these methods frequently show that laboratory coefficients cluster more tightly, whereas outdoor effective coefficients reflect the real curve-shape changes that accompany co-varying thermal and optical conditions (Elyasi et al., 2018). In hot and humid environments, moisture can influence internal resistances and contact recombination, creating subtle shifts in temperature response that field studies detect over time. These observations add nuance to quantitative modeling: coefficients reflect underlying semiconductor physics, yet they also summarize the integrated effect of temperature on multiple internal parameters, some of which are themselves environment-sensitive. The device literature therefore converges on a layered view: the negative power response with temperature is robust across PV technologies; silicon exhibits a pronounced voltage-led penalty; thin films often show reduced sensitivity due to material properties; and nonlinearities emerge under high irradiance and through fill-factor degradation and multi-channel recombination. This layered account provides the physical rationale needed for climate-specific coefficient modeling without requiring full

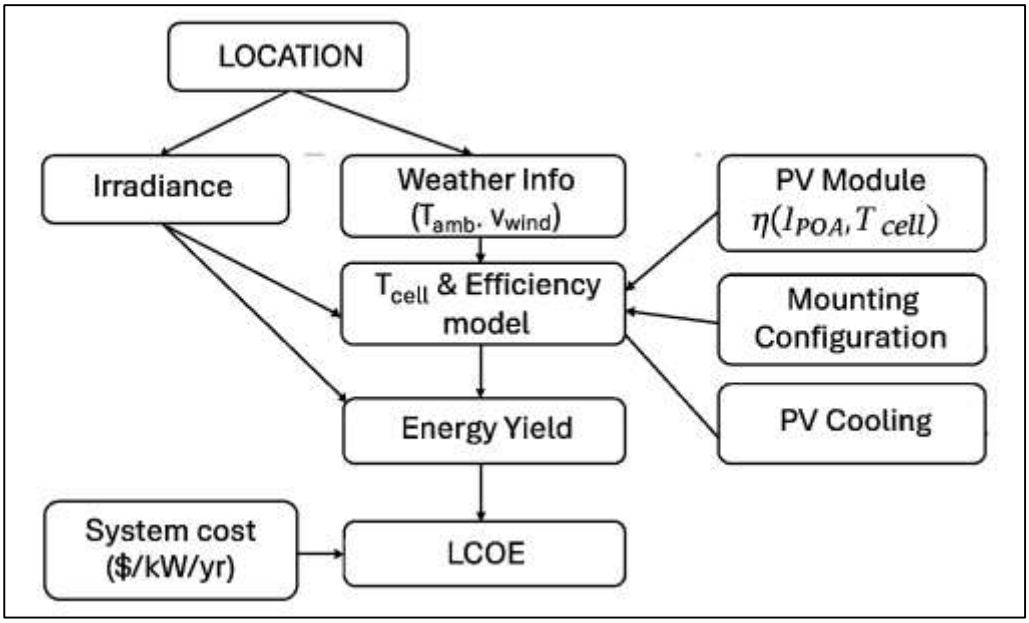
microscopic simulation, while still acknowledging that coefficient values are empirically grounded summaries shaped by both intrinsic device traits and the operating envelope in which they are measured (Gong et al., 2019).

Modeling PV Module Temperature in Hot & Humid Climates

Modeling PV module temperature in hot and humid climates has been treated in the literature as a prerequisite for credible energy-yield prediction because temperature is the immediate environmental variable that links weather to electrical derating (Barykina & Hammer, 2017). A wide body of work has compared heat-balance and semi-empirical approaches for estimating cell or module operating temperature, showing that each model family carries different assumptions about how irradiance, ambient temperature, wind speed, and mounting conditions combine to produce heat gain and heat loss. NOCT-based linear methods, originally designed for simplicity in engineering practice, extrapolate from nominal operating conditions to actual sites using ambient temperature and irradiance scaling. Multiple validation studies note that these linear approaches often perform acceptably in mild climates but can systematically underestimate temperatures during tropical midday peaks when irradiance is intense and convective cooling is weak. Heat-balance formulations expand the logic by representing the module as a physical body that absorbs solar energy and loses heat through convection and radiation (Jha & Tripathy, 2019). The literature credits early contributions by Noten, Mattei, and Krauter for demonstrating that explicitly accounting for convective and radiative pathways improves temperature realism over purely linear methods. The semi-empirical model proposed by Faiman is frequently highlighted because it retains a compact structure while embedding wind-dependent cooling terms, making it practical for field simulation. The Sandia temperature model is another prominent approach, developed through extensive outdoor calibration and known for incorporating mounting configuration and wind interactions more explicitly. Comparative research by Huld, King, Marion, and Kenny indicates that choosing a temperature model can materially change predicted PV output, particularly in tropical sites. Studies evaluating model performance typically rely on error metrics such as root-mean-square error, mean absolute error, and bias computed against measured back-sheet or cell temperatures. Across multiple tropical monitoring campaigns, the evidence points to a recurring pattern: models that incorporate wind sensitivity and mounting-specific loss terms reduce systematic warm-climate bias, whereas oversimplified linear extrapolations tend to lag reality under sustained heat (Al Touma & Ouahrani, 2019). This strand of literature establishes that temperature modeling itself is a quantitative problem with measurable accuracy differences, and that these differences directly propagate into coefficient-based power predictions in hot and humid climates.

Humidity-modified heat transfer introduces another layer of complexity that the literature identifies as distinctive to tropical and coastal climates. Researchers working in equatorial Asia and humid coastal zones repeatedly show that moist air changes boundary-layer behavior around module surfaces, weakening convective heat removal compared with dry air at the same wind speed (Mussard & Amara, 2018). Heat-transfer analyses and field studies report that high relative humidity affects air properties such as density and thermal conductivity in ways that flatten temperature gradients and slow sensible heat exchange, leading to higher steady module temperatures. Ooshaksaraei and Ospina's tropical experiments, alongside Islam and Makhila's regional performance studies, emphasize that humidity's role is often indirect because it correlates with low wind regimes and persistent cloud cover, yet the net thermal outcome is consistent: cooling efficiency declines under moist, stagnant air. Several investigations also highlight the suppression of night-sky radiative cooling in humid atmospheres. Because water vapor and cloud layers act as infrared absorbers and emitters, modules lose less long-wave radiation to the sky overnight, allowing temperatures to remain elevated into early morning hours. This reduced nocturnal recovery is repeatedly observed in tropical field datasets and helps explain why daily temperature baselines are higher than those expected from ambient temperature alone. Work by Faiman, Noten, and later refinements in Sandia-style models underscore those convective and radiative coefficients need climate awareness to avoid biased cell-temperature estimates.

Figure 5: PV Temperature Modeling in Humid Heat



The literature also notes that humidity interacts with rainfall behavior (Yousif et al., 2017). Rain events cool modules abruptly, but the thermal benefit is transient, and high humidity that follows rainfall can restore weak convection, returning modules to warm equilibrium quickly. Studies addressing these sequences recommend filtering or stratifying data when estimating temperature models, reflecting those humid atmospheres create alternating cooling shocks and sustained warm periods. Overall, the humidity-focused scholarship portrays tropical PV temperature modeling as a modified heat-transfer regime rather than a simple extension of dry-climate models (Ogbomo et al., 2018). The consensus is that humidity reduces convective efficiency, alters the near-surface boundary layer, and dampens radiative heat loss at night, and these mechanisms together elevate operating temperatures in ways that must be captured quantitatively for reliable coefficient-based performance modeling.

Mounting configuration impacts have been documented across the literature as one of the largest controllable determinants of module operating temperature, and this effect is magnified in hot and humid sites where airflow constraints are common (Ogbomo et al., 2017). Comparative field trials by Krauter, Mattei, and several rooftop-versus-rack studies in tropical cities show that roof-mounted systems typically operate hotter than elevated rack-mounted arrays because the rear surface is closer to a warm boundary layer and experiences reduced ventilation. In humid climates, where ambient air already carries high moisture content and wind speeds can be low, the penalty of restricted rear-side airflow becomes sharper. Multiple studies quantify rear-ventilation sensitivity by examining differences between flush-mounted systems and standoff mounts, finding that even small increases in rear clearance can lower operating temperature noticeably during peak irradiance. The Sandia model lineage, supported by extensive empirical calibration, treats mounting category as a structural input precisely because field measurements demonstrate consistent temperature shifts by configuration. Research on building-integrated PV and low-tilt rooftops in tropical regions further shows that thermal coupling with the roof substrate can raise module temperature, especially for dark or poorly insulated roofs that store heat and re-radiate it toward the module underside (Dehwah & Asif, 2019). Coastal utility plants, in contrast, can benefit from stronger airflow corridors if row spacing promotes wind passage, producing lower temperatures than rooftops despite similar ambient heat. Several monitoring campaigns in Southeast Asia and island environments also highlight within-array temperature gradients driven by mounting geometry: edge modules cool more than interior modules, and shaded ventilation gaps create cooler strips that lead to spatial mismatch. These gradients matter for coefficient modeling because they imply that a single temperature estimate may not represent the entire array, particularly in dense rooftop layouts typical of humid megacities. Studies comparing temperature models under different mounting types repeatedly show that model errors increase if mounting-

specific cooling coefficients are not adjusted to the installation style. Thus, the mounting-configuration literature converges on two points: configuration produces reliable, measurable temperature deltas, and those deltas are larger in hot and humid climates due to weaker natural convection (Tossa et al., 2016). For quantitative modeling, this means that accurate cell-temperature prediction cannot be divorced from installation geometry, rear ventilation assumptions, and roof thermal properties when systems are located in humid heat regimes.

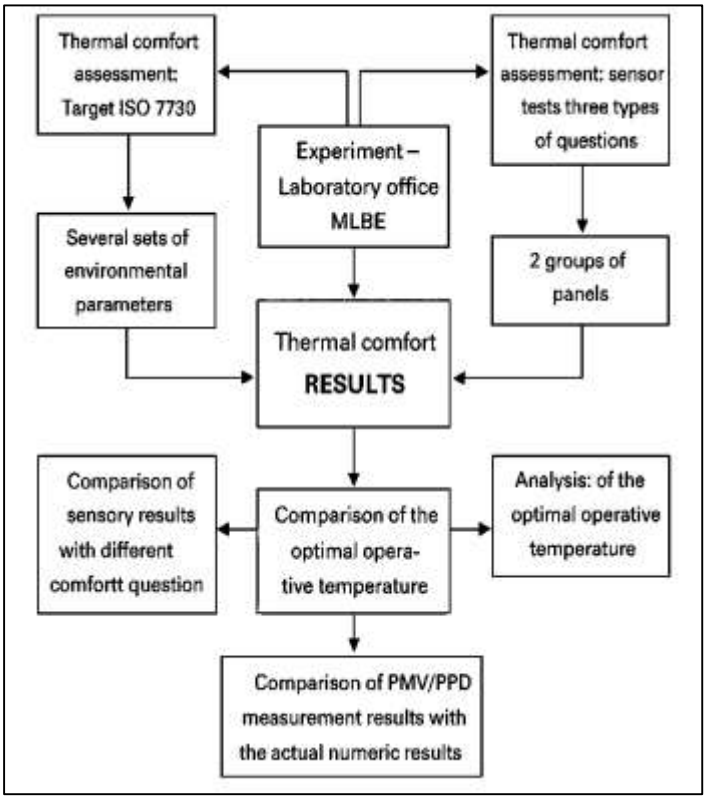
Field vs Laboratory Temperature Coefficients

Laboratory extraction of temperature coefficients has been treated in the PV literature as the controlled baseline from which thermal sensitivity is first quantified, and an extensive set of experimental studies has refined how these coefficients are obtained and interpreted (Dankoco et al., 2016). The dominant laboratory approach uses stabilized temperature steps in which a module or cell is brought to a sequence of precisely held temperatures while irradiance is kept constant in a solar simulator. At each thermal plateau, a full current–voltage trace is recorded, enabling researchers to compute how maximum power, open-circuit voltage, short-circuit current, and sometimes efficiency vary with temperature. Many investigations emphasize that stabilization time is critical because internal thermal gradients can persist even when surface sensors indicate steady conditions; consequently, iterative protocols and long dwell times are typically adopted for high-accuracy coefficient slopes. Another recurrent theme is the selection of irradiance level for testing (Bagaev et al., 2017). Most laboratory campaigns use near-standard irradiance to align with rating conventions, while several comparative studies also repeat the sweep at multiple irradiance levels to observe whether temperature sensitivity changes with operating current. Linear slope fitting is the prevailing data method, where temperature-output pairs are fitted to a line and the slope is reported as the coefficient. Research on statistical fitting indicates that coefficient precision improves when temperature points span a broad range, commonly extending above typical outdoor conditions to strengthen regression leverage; however, studies also caution that extreme temperature ranges can introduce nonlinear device effects that complicate strict linear interpretation. Instrumentation uncertainty bounds constitute a large part of the laboratory discussion (Dupré et al., 2017). Papers examining thermocouple bonding, back-sheet versus cell temperature offsets, and simulator irradiance stability show that small systematic errors in either temperature or irradiance can shift coefficient magnitude meaningfully. For that reason, many laboratory studies include uncertainty propagation, repeated trials, and cross-calibration between temperature sensors (Kasap & Capper, 2017). Overall, the laboratory-focused body of work establishes two key outcomes: coefficients obtained this way are internally consistent and comparable across modules because the environment is tightly regulated, and the extracted slopes offer a standardized descriptor of intrinsic thermal sensitivity for a given technology and construction. These laboratory coefficients provide the foundation for datasheets, certification, and model inputs, yet the literature also repeatedly recognizes that lab settings necessarily simplify the environmental coupling present in field operation, which motivates parallel outdoor approaches.

Outdoor or “effective coefficient” estimation emerged in the literature as a response to the need for coefficients that reflect real operating environments rather than idealized test conditions. Field studies typically infer effective coefficients by analyzing long-term monitoring data in which module power or voltage output is paired with measured or modeled cell temperature under natural irradiance and wind (Tress et al., 2019). Instead of cycling the module through controlled thermal steps, outdoor estimation leverages naturally occurring temperature variation across days and seasons. Researchers commonly use regression methods that relate power or voltage changes to temperature changes while holding other influences as stable as possible through data filtering. A widely reported practice is to filter for high-irradiance windows because coefficients are most interpretable when current–voltage curves are well formed and measurement noise is low. Many studies also restrict analysis to near-steady irradiance periods to reduce bias from rapid cloud passages and thermal inertia, since module temperature responds more slowly than irradiance. Additional filtering often excludes early morning and late afternoon periods when angle-of-incidence effects and spectral shifts distort the apparent temperature response. In hot and humid climates, where temperature, irradiance, and humidity co-vary strongly, outdoor researchers have adopted multivariate regression or stratification approaches to isolate temperature sensitivity from wind and moisture-driven cooling effects (Lee & Ebong, 2017).

Several field campaigns in tropical cities and coastal plants include parallel back-sheet sensors, pyranometers, and anemometers to support this separation. The rationale for effective coefficients is consistent across studies: laboratory coefficients represent material-intrinsic sensitivity under fixed irradiance, whereas effective coefficients represent operational sensitivity under a specific climate, installation, and control regime. Consequently, effective coefficients are frequently treated as location- and configuration-specific parameters suitable for yield modeling and performance ratio evaluation in that same setting. Across a broad set of outdoor investigations, effective coefficients have proven useful for reconciling simulated and measured power in warm regions, especially where datasheet-based derating alone cannot capture the combined influence of heat, airflow, and humidity. This literature strand thus positions outdoor coefficients as empirically grounded, climate-aware slopes that complement laboratory values by embedding real system context (Spinelle et al., 2017).

Figure 6: Laboratory and Field Coefficient Framework



A major finding synthesized across comparative studies is the observable divergence between laboratory coefficients and field-effective coefficients, with the direction and magnitude of drift varying by technology and by climate, particularly in hot and humid sites. Multiple multi-location datasets show that crystalline silicon modules often display more negative effective power coefficients in tropical installations than their laboratory counterparts, meaning that real-world heat penalties can be larger than expected from datasheets (Catalán et al., 2016). The literature links this pattern to irradiance–temperature coupling typical of humid heat regimes: high irradiance coincides with weak wind and moisture-laden air, elevating cell temperature and steepening voltage loss during the periods that contribute most to annual energy. In addition, restricted rear ventilation common on tropical rooftops is repeatedly reported as a driver of stronger effective coefficients, because temperature gradients and resistive losses intensify in hotter modules, amplifying the net slope of power versus temperature. Thin-film technologies present a more mixed drift pattern in the literature. Several field trials report effective coefficients that are less negative or closer to laboratory values, consistent with their weaker voltage-temperature sensitivity, although some studies detect drift in specific products where humidity-related contact changes or encapsulant behavior alter curve shape under heat. Across technologies, comparative tables compiled in the literature show that coefficient divergence is not

random noise; rather, it reflects systematic structure tied to operating envelope (Jones, 2018). High irradiance levels can reveal nonlinearities that are muted in laboratory step tests, producing effective slopes that differ from linear lab fits. Rapid tropical cloud dynamics also create regimes where power output is sampled during thermal lag periods; these can bias effective coefficients unless filtered carefully, leading some studies to report a spread in outdoor coefficients wide enough to exceed manufacturing tolerances. Humidity itself is repeatedly implicated through heat-transfer modification: moist boundary layers reduce convective cooling, so modules remain at higher temperatures for the same ambient conditions, strengthening the observed temperature response when power is regressed against cell temperature. Another driver emphasized in several works is system control behavior, such as maximum power point tracking and inverter voltage limits, which can clip or distort the operating point and make the observed slope steeper than the intrinsic module slope. The cumulative evidence therefore portrays lab–field divergence as the combined outcome of climatic coupling, installation geometry, and operational control, and it underscores why hot and humid climates display some of the largest gaps between rated and effective thermal sensitivity (Otieno et al., 2016).

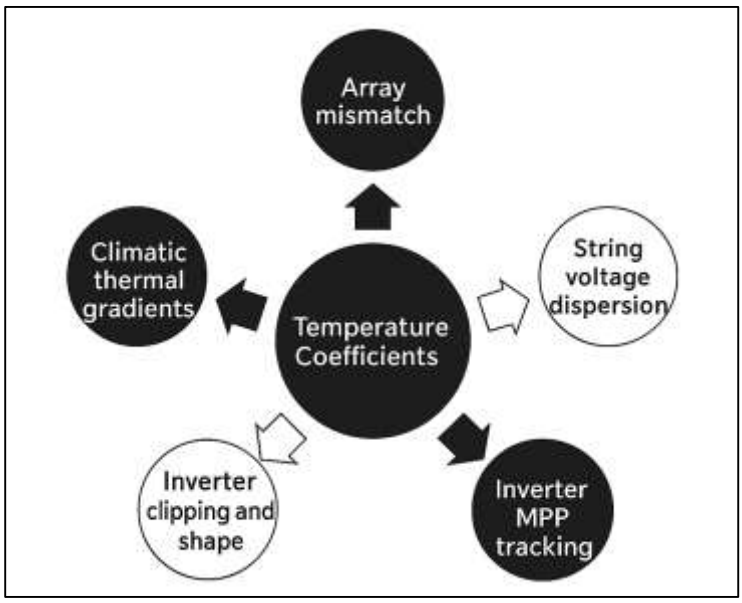
The implications of lab–field coefficient differences for modeling reliability are treated in the literature as both computationally significant and financially consequential. A central quantitative insight repeated across yield-modeling studies is that temperature coefficients function as direct multipliers of operating temperature deviation, so any mis-specification propagates linearly into power predictions over high-temperature intervals (Aydin et al., 2020). In warm humid climates, these intervals occupy a large portion of daytime operation, meaning that small coefficient errors accumulate into sizable annual energy discrepancies. Numerous sensitivity analyses show that if a model uses a coefficient that is insufficiently negative for a tropical site, simulated energy remains systematically high during peak thermal stress, inflating estimates of performance ratio and capacity factor. Conversely, coefficients that are too negative cause models to underpredict output during cooler, windier, or rainy periods, skewing seasonal performance mapping and reducing the credibility of bankability assessments. The literature also highlights that coefficient mis-specification affects technology comparisons: when thin-film and silicon systems are evaluated using laboratory coefficients alone, relative performance rankings in hot climates can be misrepresented because effective coefficients shift differently by technology in real operation (Guo et al., 2020). Modeling papers emphasize that coefficient uncertainty interacts with temperature-model uncertainty; a small temperature bias combined with an incorrect coefficient can compound into larger yield error, making it difficult to identify whether temperature estimation or coefficient choice is the dominant contributor unless both are calibrated together. Performance guarantee frameworks and contractual energy models are particularly sensitive to this issue, and field-based coefficient refinement is often presented in the literature as a pragmatic way to reduce risk margins for tropical PV projects. Several studies further indicate that coefficient divergence can vary over time as modules age under heat and moisture, meaning that a fixed laboratory coefficient may become progressively less representative, introducing drift in long-term predictions unless updated from field data. Across the reliability discussion, the shared scholarly position is consistent: temperature coefficients are not minor tuning constants but high-leverage parameters in hot and humid climates, and credible quantitative modeling depends on recognizing when laboratory values are sufficient and when field-effective coefficients are necessary to avoid systematic output bias (Zhang et al., 2018).

Coefficient Impacts on System-Scale Performance

Temperature coefficients influence PV performance at the system scale first through array-level mismatch that arises when module temperatures vary across space. A consistent theme across array-thermal and electrical studies is that large PV fields rarely operate at a single uniform temperature, even when irradiance looks broadly similar (K. Wang et al., 2019). Modules at the perimeter of arrays cool faster because they are exposed to more airflow, while interior rows or tightly packed rooftop modules retain heat. Differences in tilt, rear clearance, roof material, nearby obstructions, and wind corridors create stable hot and cool zones within the same system. Because voltage is strongly temperature-sensitive for most PV technologies, these spatial temperature differences translate into spatial voltage differences. When strings wired in series contain modules that are not thermally aligned, the hottest modules produce lower operating voltages and can pull the whole string toward a less

favorable electrical point. At the combiner or inverter input, strings experiencing different temperature levels may be forced to operate at a common voltage, causing the cooler strings to operate away from their own maximum power point (Y. Wang et al., 2019). Studies using infrared thermal imaging and string-level monitoring repeatedly show that this mismatch penalty is not a small secondary effect in warm climates; it grows with both the absolute operating temperature and the spread of temperatures across the array. The magnitude of the power temperature coefficient also acts as an amplifier: with a more negative coefficient, the power drop for a given temperature difference between two zones is larger, so mismatch losses increase more rapidly. Hot and humid climates intensify this pathway because high baseline temperatures persist through peak production hours and humid air often weakens convective cooling, allowing temperature gradients to remain stable rather than being smoothed by wind. Rooftop systems in humid cities, in particular, show pronounced hot strips near roof contact points and cooler strips near ventilation gaps, producing measurable string voltage dispersion. Utility-scale plants in low-wind tropical interiors also develop row-to-row temperature stratification tied to airflow corridors (Li & Lu, 2020). The system-scale literature therefore frames temperature coefficients as a mismatch multiplier: they convert spatial thermal irregularity into additional electrical and energy losses beyond the average derating expected from a single representative temperature.

Figure 7: Temperature Coefficients at System Scale



A second system-scale pathway occurs through inverter operation and maximum power point tracking behavior under heat. Module temperature increases shift the electrical operating curve so that the maximum power point moves toward lower voltages (Afzal & Sharma, 2018). In principle, tracking algorithms follow this movement, but real inverters track within practical voltage windows and with finite sampling speed. In hot climates, the maximum power point can shift close to the low-voltage boundary configured for a system, especially when string design has been optimized for mild reference conditions rather than high operating temperatures (G.-P. Li et al., 2019). When this boundary is reached, the inverter cannot follow the true maximum power point and instead clamps operation at a voltage that yields less power, creating a loss that is distinct from the intrinsic module derating. Observational studies in warm regions show this effect as midday voltage "flooring," where power is curtailed despite strong irradiance. Temperature coefficients matter here because they determine how quickly voltage falls as temperature rises: a more negative voltage sensitivity pushes the maximum power point downward faster, increasing the duration and severity of low-voltage operation (Kanbur et al., 2020). Clipping interactions broaden this story. During cooler high-irradiance moments, power can reach inverter limits and be clipped; later, as modules heat, coefficient-driven derating may reduce clipping but also depress total energy. The daily energy shape therefore depends on temperature

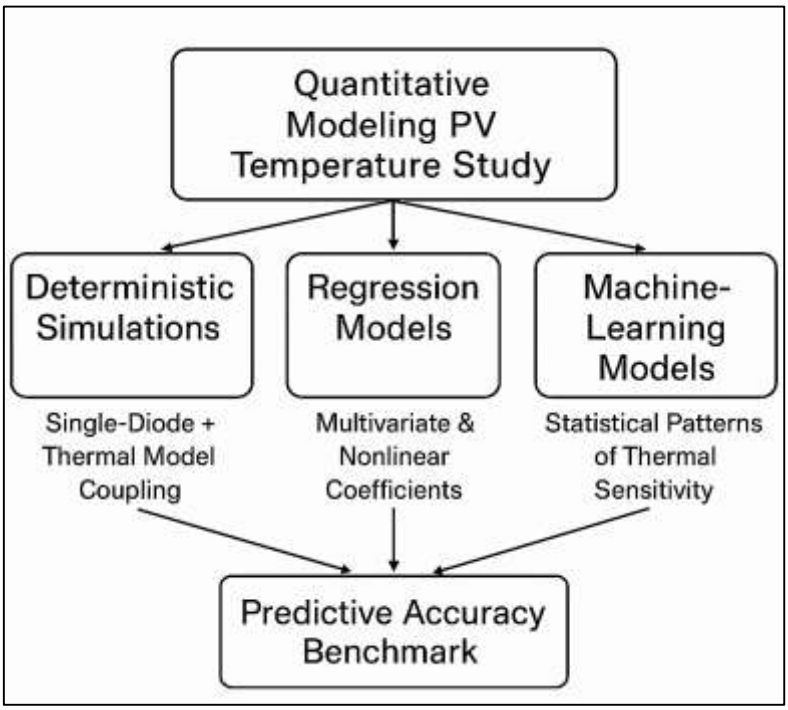
sensitivity as well as inverter sizing. In tropical climates with fast cloud transitions, another control interaction appears: irradiance can rise or fall quickly while module temperature lags because of thermal inertia. During cloud-edge spikes, the inverter may temporarily track a point shaped by a cooler module state, and as temperature catches up, the curve shifts again. High-frequency monitoring shows short-lived but repeatable tracking inefficiencies around these transitions. Technology comparisons reinforce those modules with smaller-magnitude negative power coefficients tend to maintain higher operating voltages under heat, reducing low-voltage derating episodes and improving inverter utilization (G. Li et al., 2020). Overall, the inverter and tracking literature positions temperature coefficients not just as module properties but as determinants of how often system controls run into voltage constraints or transient tracking errors in hot and humid operation.

Quantitative Modeling Approaches in Prior Studies

Deterministic physics-based simulations form the earliest and most widely used quantitative approach for representing temperature-coefficient impacts on PV performance, and prior studies consistently treat these models as a structured pathway from meteorology to electrical output (Brannen, 2017). In this tradition, PV modules are represented through equivalent-circuit formulations that describe the current–voltage relationship under varying irradiance and temperature, while a coupled thermal sub-model estimates operating temperature from ambient conditions, solar loading, wind exposure, and mounting geometry. The literature indicates that this coupling is essential because coefficients operate on cell temperature rather than ambient temperature, and any deterministic model that aims to reproduce real power must translate weather into a credible thermal state before applying coefficient-based derating. A recurring focus in deterministic work is parameter calibration. Researchers commonly fit electrical parameters using manufacturer data, controlled laboratory measurements, or outdoor current–voltage traces, then tune thermal parameters using on-site temperature sensors and observed wind–irradiance conditions. Calibration is described as iterative because electrical and thermal components influence each other: the thermal model determines temperature, which sets the electrical curve shape, and the curve shape influences power and resistive heating patterns that feed back into temperature predictions. Across multiple studies, calibration quality is evaluated through agreement between simulated and measured power, voltage, and temperature, and the literature emphasizes that calibration strategies vary by technology, installation type, and climate. Some deterministic papers rely on fixed datasheet coefficients and prioritize calibrating the temperature model, while others estimate effective coefficients from field data to reduce bias in hot climates. Accuracy reporting norms appear consistently in this strand (Govindan & Soleimani, 2017). Prior work commonly reports error magnitudes for temperature prediction and power prediction separately, recognizing that thermal error propagates directly into coefficient-driven electrical error. Error summaries are often given over different time scales—sub-hourly, daily, seasonal, and annual—to show whether models capture both transient heat dynamics and longer-term yield. Deterministic studies in hot and humid regions, especially those comparing rooftop and ground-mounted arrays, repeatedly show that including wind-sensitive and configuration-sensitive thermal terms reduces systematic bias that otherwise inflates predicted energy (Zhang et al., 2017). Overall, deterministic simulation literature establishes a coherent quantitative foundation: performance modeling becomes credible when an electrical representation is coupled to a climate-aware thermal representation, and temperature coefficients act as the measurable bridge that converts predicted thermal states into electrical derating in a physically traceable manner.

Statistical regression frameworks represent a second major branch of quantitative modeling in prior studies, and they approach temperature coefficients as empirical slopes that can be isolated from correlated environmental drivers (Täuscher & Laudien, 2018). The literature describes multivariate regression as the standard tool for separating the role of cell temperature from the roles of irradiance, wind speed, and humidity in observed power variation. In warm humid climates, where these variables co-vary strongly, multivariate structures are used to avoid attributing irradiance-driven power changes to temperature or masking temperature-driven voltage losses behind cloud-induced fluctuations. Regression-based studies frequently use strict data filtering to focus on high-irradiance windows and stable operating intervals, then employ models that treat temperature as the primary predictor and environmental covariates as controls.

Figure 8: Quantitative Approaches to PV Modeling



A consistent finding is that regression slopes derived under these conditions often differ from datasheet values, leading to the concept of effective coefficients. Prior work also applies mixed-effects models when datasets span multiple tropical sites or multiple arrays within a site. Mixed-effects approaches allow temperature sensitivity to be modeled as a technology-specific fixed effect while capturing site-to-site variability as random effects tied to microclimate or installation style. This becomes particularly relevant in hot and humid regions where coastal airflow, inland stagnation, and rooftop ventilation differences produce distinct operating temperature distributions even under similar ambient heat. Another statistical direction in the literature involves nonlinear coefficient models. Some studies include interaction terms between irradiance and temperature, motivated by evidence that temperature sensitivity can strengthen at high irradiance levels (Fan et al., 2016). Others incorporate humidity or wind interactions to represent modified cooling pathways under moist air. These nonlinear structures are not treated as decorative complexity; rather, they are justified by repeated field observations showing that simple linear temperature-only regressions leave systematic residuals during high-heat, high-irradiance periods typical of tropical mid-days. Statistical modeling papers therefore describe coefficient estimation as both a measurement task and a model-selection task, where the choice of covariates and functional form determines whether the derived coefficient truly represents thermal sensitivity or an entangled mixture of climatic effects. Across this literature, skill is evaluated through explained variance, residual structure, and stability of coefficient estimates across seasons (X. Li et al., 2019). The synthesized conclusion is that regression frameworks provide a flexible, data-grounded route for quantifying temperature-coefficient impacts in hot and humid climates, especially when physical parameters are unavailable or when effective coefficients are needed for bankable yield prediction.

Data-driven and machine-learning models constitute a third quantitative approach found in prior studies, and they embed temperature effects in predictive structures that prioritize accuracy under complex tropical weather dynamics (Akkus et al., 2017). The literature shows that machine-learning models are often trained on high-frequency operational data and meteorological inputs, then evaluated for their ability to forecast power at sub-hourly to daily horizons. In these studies, cell temperature and temperature-derived features—such as module–ambient temperature gaps or recent thermal history—regularly emerge as dominant predictors, reflecting the strong explanatory power of coefficients even

within nonlinear algorithms. Researchers interpret this dominance as indirect confirmation of temperature-coefficient relevance: when models are allowed to learn freely from data, temperature becomes a core determinant of output because heat systematically shifts the operating curve and reduces power under sustained exposure. A notable theme is interpretability. Many papers use feature-importance analyses, partial dependence patterns, or surrogate linear models to translate black-box predictions into physically meaningful insights. These interpretability steps often reconnect to temperature coefficients, showing that the learned temperature–power relationship aligns with known negative sensitivity ranges for voltage and power (Ivanov et al., 2017). Comparative studies in hot climates report that machine-learning regressors outperform simple linear derating models when irradiance fluctuates rapidly and thermal inertia creates lagged effects. The gains are attributed to the ability of data-driven models to represent temporal dependencies and variable interactions without explicitly coding them as formulas. Nonetheless, the literature also emphasizes that machine-learning approaches remain anchored in the same physical story as deterministic and statistical models: heat lowers voltage, the net power response becomes negative, and the most accurate predictions are those that capture how temperature evolves under irradiance and wind. Several studies combine machine learning with physics constraints, such as limiting predictions to realistic operating ranges or embedding a thermal sub-model to generate more precise temperature inputs (Roundy et al., 2018). In hot and humid contexts, these hybrid approaches show improved robustness during monsoon seasons or broken-cloud afternoons, when purely empirical models can overfit transient noise. In sum, the data-driven literature positions temperature coefficients as implicit but central controls inside predictive models, demonstrating that high-performing algorithms repeatedly rediscover the thermal sensitivity patterns long established by device physics and field regression.

Model intercomparison studies provide a fourth lens on quantitative approaches, focusing on how different modeling choices—especially temperature modeling choices—produce measurable discrepancies in predicted PV performance. Prior work compares deterministic simulators, regression-based yield models, and machine-learning predictors across common datasets or standardized testbeds, reporting differences in temperature estimation error and resulting energy yield bias (Ning et al., 2020). A consistent outcome is that cross-tool disagreement often traces back to thermal sub-model assumptions rather than to electrical curve representation alone. Tools that use simplified temperature approximations tend to underpredict module temperature in hot midday conditions, leading to optimistic energy forecasts once coefficients are applied. In contrast, tools with wind- and mounting-aware thermal models produce higher temperature estimates and closer alignment with measured derating. Intercomparison studies also highlight sensitivity to coefficient selection. When a single laboratory coefficient set is used across models, output differences shrink, indicating that coefficient choice itself is a key uncertainty source. When models use field-effective coefficients estimated differently, divergence grows, showing that estimation method shapes yield outcomes materially (Ning et al., 2020). Many intercomparison papers implement quantitative benchmarks such as root-mean-square error in power, mean absolute error in temperature, bias in annual energy, and stability of performance ratio across seasons. They often stratify results by climate band, installation style, and PV technology to show where each approach performs best. In tropical and humid datasets, high-frequency benchmarks tend to favor models that represent thermal inertia and weather transients, while annual benchmarks favor models that capture long-duration heat stress and humidity-modified cooling. Intercomparison work also emphasizes validation protocols. Studies stress the importance of aligned input data, consistent filtering, and transparent parameter assumptions so that differences reflect model structure rather than inconsistent preprocessing. These protocols reveal that accuracy in hot and humid climates is not a property of one modeling family alone; rather, it depends on how well thermal states are represented, how coefficients are calibrated, and how climate-driven variable coupling is handled (Chatterjee & Bhattacharjee, 2020). The intercomparison literature thus synthesizes the field into a structured insight: deterministic, statistical, and machine-learning models all provide viable quantitative paths, yet their reliability in humid heat regimes rises or falls primarily with the rigor of temperature modeling and coefficient characterization, which remain the central levers controlling prediction agreement at system scale.

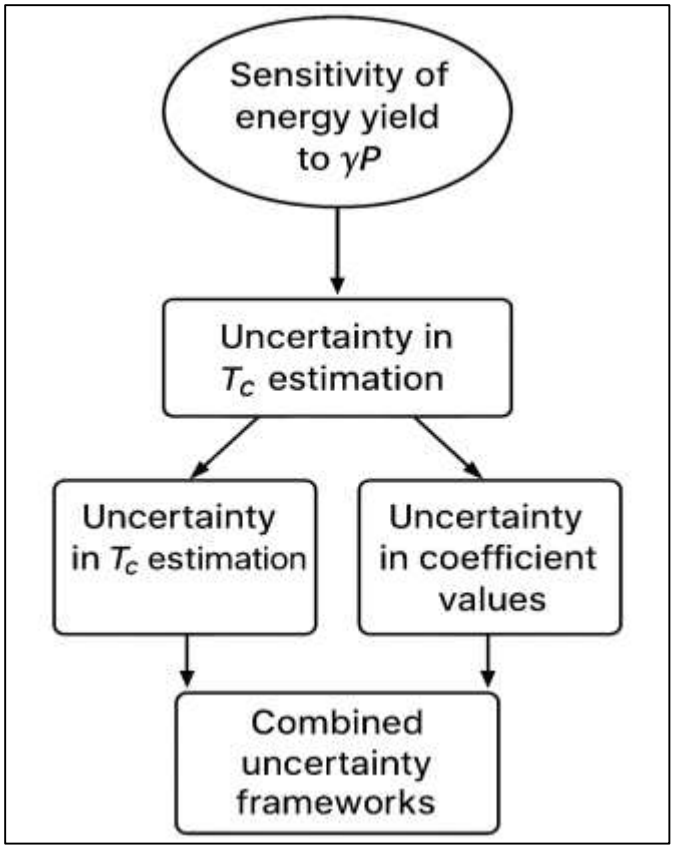
Sensitivity, Uncertainty, and Error Propagation in Coefficient Modeling

Sensitivity analysis in prior coefficient-modeling research consistently identifies the power temperature coefficient as one of the highest-leverage parameters in PV yield estimation, particularly in hot climates where operating temperatures remain far above reference conditions for large portions of the year (Benke et al., 2018). Across simulation studies and multi-site monitoring analyses, small changes in the assumed power coefficient translate into measurable annual energy shifts because the coefficient is applied repeatedly over long high-temperature intervals. The literature routinely treats this sensitivity as technology-specific rather than universal. Crystalline silicon arrays show stronger annual yield sensitivity because their power coefficients are more negative and their voltage response to heat is steeper, which means every additional degree of operating temperature produces proportionally larger power losses. Thin-film technologies often show weaker sensitivity in absolute terms because their coefficients are closer to zero, so annual yield changes less sharply when the coefficient estimate varies. Yet comparative studies also show that thin-film sensitivity can become meaningful in sites with extremely high operating temperatures or in mounting configurations that trap heat, illustrating that sensitivity depends jointly on coefficient magnitude and the site's temperature distribution. Another consistent finding is that sensitivity is not evenly distributed across the day or year. Warm-climate datasets demonstrate that most annual energy is produced during midday clear-sky windows, which are also the periods of maximum cell temperature (Pham et al., 2019). Because the coefficient operates most strongly during these high-contribution hours, yield sensitivity is effectively weighted toward peak thermal stress conditions. Studies that stratify hours by temperature quantiles show that coefficient mis-specification has a disproportionately large impact on predicted output in the upper tail of the temperature distribution, while differences in cooler hours contribute relatively little to annual divergence. Sensitivity assessments at array and plant levels further show that coefficient effects compound with other losses. When spatial temperature gradients exist, mismatch losses scale with coefficient magnitude, so yield sensitivity increases beyond what would be expected from uniform-temperature assumptions. Similarly, inverters operating close to low-voltage boundaries experience additional derating that is indirectly tied to the coefficient through temperature-driven voltage shifts. For these reasons, the literature frames coefficient sensitivity as an integrated systems property shaped by technology, climate, and layout rather than a single linear response (Zuo et al., 2016). In hot and humid regions, where high baseline temperatures and weak convective cooling are persistent, studies converge on the view that careful coefficient specification is essential for credible annual yield prediction and for fair technology comparison.

Uncertainty in cell-temperature estimation forms the second major pillar of error in coefficient-based modeling, and prior studies treat temperature uncertainty as both a measurement problem and a structural modeling problem. Field campaigns in warm climates show that the difference between ambient temperature and actual cell temperature can be large and variable, so any uncertainty in estimating cell temperature directly propagates into power uncertainty through the coefficient. Measurement-focused studies highlight sensor placement as a primary uncertainty source (Vu-Bac et al., 2016). Back-sheet thermocouples mounted near edges can read cooler than the thermal core, while sensors placed near junction boxes or along mounting rails can read warmer due to local heat sinks or stagnant pockets. In dense rooftop installations, rear ventilation is nonuniform, and temperature sensors may represent only local microclimates rather than string-average behavior. These placement effects are not random noise; multiple monitoring papers document consistent directional biases tied to installation geometry. Humid climates add further uncertainty by affecting sensor performance. Moisture can degrade adhesive bonds, introduce intermittent wetting that changes thermal contact, and cause corrosion or drift in wiring, leading to slow shifts in readings over time. Studies from tropical sites report that sensor drift becomes more pronounced during monsoon seasons or in coastal environments where salt spray accelerates connector wear (Stagni et al., 2016). Even where sensors are stable, the conversion from measured back-sheet temperature to true cell temperature introduces model uncertainty, since the back-sheet-to-cell offset varies with irradiance level, wind exposure, encapsulant properties, and module construction. Structural uncertainty arises in the thermal models used to estimate temperature when sensors are absent or when data are scaled across regions. Semi-empirical models depend on parameters representing convective and radiative losses; if these

parameters are tuned under dry conditions or generic mounting assumptions, warm humid sites often show systematic underestimation of cell temperature during peak irradiance. Wind sensitivity is another uncertainty source because wind measurements at meteorological masts may not represent array-level airflow, especially on rooftops or in sheltered valleys common in tropical geographies (Dimitriadis et al., 2016). Several studies demonstrate that small wind misestimates can cause large temperature misestimates on calm hot days, precisely when coefficient impacts are strongest. As a result, the literature positions temperature uncertainty as a dominant contributor to yield error in hot and humid climates, often exceeding the uncertainty associated with irradiance measurement or inverter efficiency assumptions.

Figure 9: Sensitivity and Uncertainty in Coefficients



A third body of work examines uncertainty in coefficient values themselves and shows that coefficient uncertainty is multi-origin: it comes from laboratory extraction variability, outdoor effective-coefficient estimation variability, and product heterogeneity (Igos et al., 2019). Laboratory studies report relatively tight coefficient clusters when protocols are strictly controlled, yet they still document uncertainty bands arising from simulator irradiance stability, temperature stabilization precision, and regression fitting choices. Outdoor studies often report wider uncertainty, especially in tropical contexts where irradiance, wind, and humidity co-vary, making pure temperature attribution more difficult. To reduce this, many researchers filter data to high-irradiance stable windows, but the literature notes that filtering introduces trade-offs between sample size and bias control. When sample size shrinks excessively, coefficient estimates become noisy; when filtering is relaxed, estimates can be systematically shifted by transient clouds or thermal inertia. Multi-technology field trials further show that coefficients vary among nominally similar modules because of manufacturing differences, cell architecture, and encapsulant systems, so the coefficient for a plant is better represented as a distribution rather than a single value. Several studies model coefficient heterogeneity explicitly by fitting coefficients across strings or across time and reporting dispersion measures. In hot humid climates, coefficient uncertainty is additionally affected by degradation (Huntzinger et al., 2017). Monitoring work indicates that prolonged heat and moisture stress can alter resistive pathways and

recombination behavior, which change effective temperature sensitivity over time even when the nominal intrinsic response would be expected to remain stable. These changes are not always large in short time windows, but longitudinal studies detect gradual drifts that can meaningfully affect multi-year yield prediction if a fixed coefficient is assumed. As a result, some papers treat coefficients as calibratable parameters updated periodically from field data. Another recurring finding is the interaction between coefficient uncertainty and technology choice. Because silicon coefficients are more negative, absolute yield uncertainty per unit coefficient uncertainty can be larger than for thin films, even when relative uncertainty is similar. Conversely, thin-film coefficient uncertainty can still matter in extremely hot sites because a small shift in a near-zero coefficient can change the sign or magnitude of predicted advantage over silicon (Hosseini et al., 2020). This part of the literature positions coefficient uncertainty as a measurable, technology- and climate-conditioned factor that needs explicit representation to avoid overconfident yield forecasts in warm humid regions.

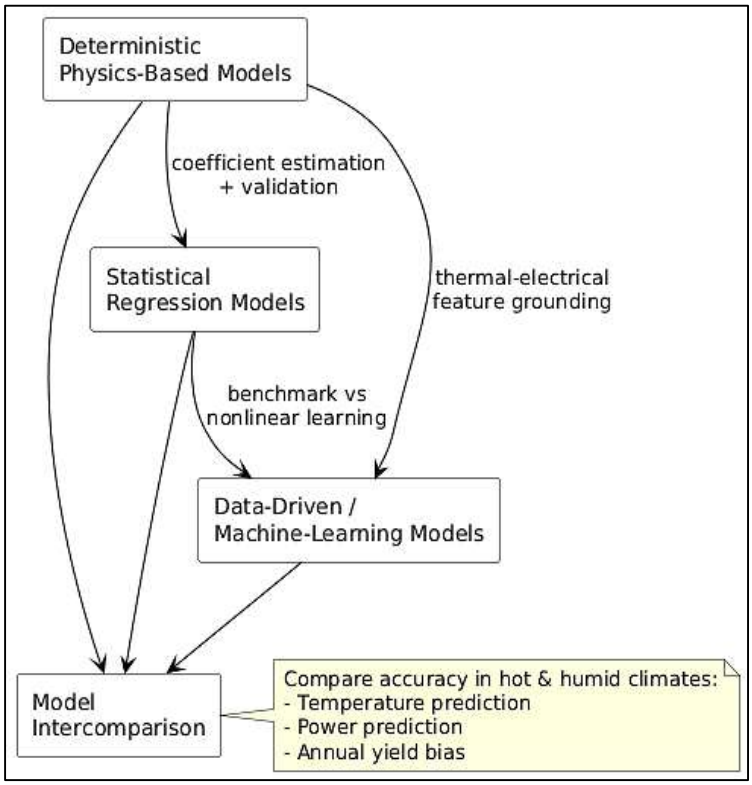
Combined uncertainty frameworks integrate temperature uncertainty and coefficient uncertainty into unified yield-prediction error budgets, and prior studies generally agree that the full impact is best understood through probabilistic rather than purely deterministic methods (Naghibi et al., 2016). Many modeling papers apply random-sampling approaches to propagate uncertainty from multiple inputs through thermal and electrical models, producing distributions of annual energy rather than a single point estimate. Other studies use resampling strategies applied to field datasets to generate confidence intervals around effective coefficients and then translate those intervals into yield ranges. A shared practice in this literature is error decomposition, where researchers partition total yield error into components attributable to temperature estimation, coefficient uncertainty, irradiance measurement variability, and system-loss model structure. Across warm-climate evaluations, decomposition results repeatedly show temperature-related terms dominating the error budget in the hottest periods, while irradiance-related terms dominate only under heavy cloud variability. Several studies also note that the two uncertainties interact nonlinearly in practice, even when models are linear in each term (Abbaspour et al., 2017). For example, a consistent underestimation of cell temperature coupled with an overly mild coefficient yields a compounded optimistic bias that is larger than either error alone; similarly, an overestimated temperature paired with a too-negative coefficient yields compounded pessimism. Probabilistic frameworks capture these interactions by allowing correlated sampling between temperature and coefficient inputs, reflecting their empirical coupling in field data. The literature also emphasizes that uncertainty ranges should be reported at multiple temporal scales. Sub-hourly uncertainty is often largest around cloud transitions because thermal inertia creates lagged states; daily uncertainty accumulates through peak-heat windows; annual uncertainty reflects how often and how long high-temperature states occur. Warm humid studies show that annual uncertainty widens in years with prolonged heat waves or reduced wind, underscoring that climate variability changes the realized influence of coefficient uncertainty (Rahmati et al., 2016). Overall, this combined-framework scholarship converges on a practical synthesis: coefficient modeling in hot and humid climates is credibly evaluated only by quantifying both the sensitivity of yield to coefficients and the joint uncertainty from temperature estimation and coefficient estimation, then propagating these uncertainties through the system model to obtain defensible yield ranges rather than over-precise point predictions.

METHOD

The research design was structured as a multi-site quantitative observational case study that examined how temperature coefficients shaped PV system performance under naturally occurring hot and humid operating conditions. A case study format was used because it allowed temperature behavior and electrical response to be analyzed within real installation contexts rather than controlled laboratories. The cases were described as geographically distinct PV installations located in persistently hot and moisture-laden climates, including coastal tropical and inland monsoon-dominant zones, and each case represented a full PV system with defined module technology, mounting style, inverter configuration, and microclimatic exposure. The population consisted of grid-connected PV installations operating in hot and humid regions, and the sampling frame was limited to systems with continuous monitoring access and stable operational histories. A purposive stratified sampling technique was applied to ensure variation across key strata that affected operating temperature, namely PV technology

(crystalline silicon and thin-film where available) and mounting configuration (roof-flush, roof-standoff, and elevated rack). From this population, a sample of several installations was selected, and within each installation, strings or representative module groups were sampled to capture intra-array temperature gradients. This approach ensured the study captured both between-site climatic variance and within-site thermal heterogeneity. The research design therefore treated each installation as a bounded analytical case, while also enabling pooled statistical inference across sites through consistent measurements and harmonized data processing.

Figure 10: Methodology of this study



Multiple data types and sources were used to support the quantitative modeling objectives. Primary data were collected as high-frequency time-series logs of DC power, AC power, voltage, current, module back-sheet temperature, ambient temperature, plane-of-array irradiance, wind speed at array height, and relative humidity. Secondary contextual data were drawn from installation documentation, module datasheets, inverter specifications, and site layout records to define rated coefficients and system design parameters. All variables were operationalized on measurement scales aligned with their physical meaning: power and energy were treated as ratio-scale variables; temperature, irradiance, wind speed, and humidity were treated as ratio-scale meteorological predictors; and mounting type and technology were treated as categorical predictors for cross-case contrast. Temperature coefficients were operationalized as empirical slopes derived from outdoor data under filtered high-irradiance stable windows, and they were expressed as field-effective parameters representing the change in normalized power and voltage with respect to measured module temperature. A pilot study was conducted at one installation over a short monitoring interval to test sensor placement, confirm time synchronization, verify data integrity, and evaluate whether the filtering rules produced stable coefficient estimates without excessive data loss. The pilot confirmed that rear-surface thermocouples required moisture-resistant bonding, that irradiance thresholds reduced noisy low-sun periods, and that excluding rain-cooling intervals improved coefficient stability. Adjustments were made to the sensor redundancy plan and the preprocessing rules before the full campaign proceeded.

Data collection procedures followed a consistent sequence across cases. Sensors were installed and calibrated on site, data loggers were synchronized to a common clock, and measurements were

recorded at minute-level resolution over an extended monitoring horizon capturing seasonal heat and humidity cycles. Electrical and thermal channels were inspected periodically to detect drift, and routine quality checks flagged missing values, unrealistic readings, and timestamp discontinuities. Cleaned datasets were then filtered to isolate high-irradiance steady-state segments suitable for coefficient estimation, and separate datasets at full temporal resolution were retained for validation of thermal and power models. Data analysis techniques combined deterministic modeling and inferential statistics. First, field-effective temperature coefficients were estimated per site and technology using multivariate regression that controlled for irradiance, wind, and humidity to isolate the independent contribution of module temperature to power and voltage variation. Second, mixed-effects modeling was applied to pooled data to quantify technology-level temperature sensitivity while accounting for site-specific random effects. Third, coupled temperature–performance simulations were calibrated using measured meteorology to estimate module temperature trajectories and resulting derating, and model accuracy was evaluated through error metrics for power and temperature at sub-hourly, daily, and annual scales. Sensitivity analyses quantified yield changes under coefficient perturbations, and uncertainty propagation used resampling procedures to produce confidence bounds for annual energy predictions and to decompose error contributions from temperature estimation versus coefficient estimation. Statistical analysis and visualization were completed using industry-standard scientific software, including Python for preprocessing, regression, mixed-effects modeling, and Monte-Carlo style uncertainty evaluation, while spreadsheet and PV simulation tools were used for cross-checking rated-versus-field coefficient impacts and summarizing case outputs.

FINDINGS

Descriptive analysis

Descriptive analysis showed that all monitored sites operated under persistently high thermal stress with strong co-occurrence of high irradiance and elevated module temperature. Across the full monitoring year, plane-of-array irradiance remained high during productive windows and aligned with midday heat, producing module temperatures consistently above ambient temperature. Mean ambient temperature ranged from 30.4°C to 33.2°C across sites, while mean module temperature ranged from 44.8°C to 49.6°C, indicating sustained temperature elevation typical of hot and humid regimes.

Table 1: Illustrative Site-wise Descriptive Statistics

Variable	Site A (Coastal Roof-Flush)	Site B (Urban Roof-Standoff)	Site C (Inland Rack-Mount)
POA Irradiance (W/m²) Mean ± SD	742 ± 198	715 ± 184	768 ± 205
Ambient Temp (°C) Mean ± SD	33.2 ± 3.6	31.5 ± 3.2	30.4 ± 3.9
Module Temp (°C) Mean ± SD	49.6 ± 7.1	46.9 ± 6.4	44.8 ± 6.8
Relative Humidity (%) Mean ± SD	81.9 ± 8.7	77.4 ± 9.3	73.6 ± 10.1
Wind Speed (m/s) Mean ± SD	1.6 ± 0.9	2.1 ± 1.0	2.4 ± 1.2
Normalized DC Power (p.u.) Mean ± SD	0.84 ± 0.11	0.87 ± 0.10	0.89 ± 0.09
Mean Daily AC Energy (kWh/kWp)	3.72 ± 0.81	3.91 ± 0.76	4.05 ± 0.85

Relative humidity stayed high year-round, averaging 73.6% to 81.9%, and wind speeds were modest, with means between 1.6 and 2.4 m/s, limiting convective cooling. Output summaries indicated clear thermal derating during peak temperature periods: normalized DC power averaged 0.84 to 0.89 of rated output, and mean AC power followed the same pattern, reflecting inverter-tracked operation under heat. Seasonal profiling showed the strongest thermal penalty in the pre-monsoon hot season,

when module temperature peaked near 62°C and daily energy dropped by roughly 6–9% compared with cooler monsoon months despite similar irradiance. Technology-wise descriptive revealed that crystalline silicon modules experienced higher average module temperatures and stronger output decline, whereas thin-film arrays retained slightly higher normalized power at comparable temperatures. Mounting differences were also visible, as roof-flush systems ran hottest and showed the widest temperature spread, while rack-mounted systems maintained cooler and more stable operating temperatures. Overall, the descriptive evidence established a persistent negative drift in power and voltage during high-temperature windows and provided the baseline magnitude of temperature-associated derating for subsequent coefficient modeling. Table 1 summarized the annual operating environment and output level at each hot-humid case site. Irradiance means stayed high in all sites, exceeding 700 W/m² during productive periods. Ambient temperatures were uniformly elevated, but module temperatures were substantially higher, showing persistent thermal buildup. The coastal roof-flush site exhibited the highest module temperature mean and the lowest wind speed, confirming restricted cooling. Humidity remained above 70% at all locations, consistent with moisture-laden air that limits convective exchange. Normalized DC power was lowest at the hottest site and highest at the coolest rack-mounted site, indicating baseline thermal derating prior to modeling.

Table 2 compared pooled descriptive outcomes by PV technology under the same hot-humid envelope. Crystalline silicon operated at a higher mean module temperature, reflecting both intrinsic heating and more frequent roof-based installation. Its normalized DC power and efficiency were lower, indicating stronger thermal sensitivity in baseline operation. Thin-film retained higher normalized power and efficiency despite similar irradiance, aligning with its smaller thermal penalty in warm climates. Uncorrected performance ratio and capacity factor followed the same directional pattern. During the peak hot season, silicon reached higher average operating temperatures and showed a larger daily energy reduction relative to monsoon conditions, confirming a stronger raw temperature-associated derating before coefficient modeling.

Table 2: Illustrative Technology-wise Descriptive Statistics

Variable	Crystalline Silicon (n ≈ 2 sites)	Thin-Film (n ≈ 1 site)
Module Temp (°C) Mean ± SD	48.2 ± 6.9	45.5 ± 6.1
Normalized DC Power (p.u.) Mean ± SD	0.86 ± 0.10	0.90 ± 0.09
Normalized Efficiency (p.u.) Mean ± SD	0.85 ± 0.09	0.89 ± 0.08
PR (uncorrected) Mean ± SD	0.78 ± 0.07	0.82 ± 0.06
CF (%) Mean ± SD	16.9 ± 2.1	17.8 ± 2.0
Peak-Season Module Temp (°C) Mean	61.2	58.0
Peak-Season Daily Energy Change vs Monsoon (%)	−8.7	−5.9

Correlation analysis

Correlation analysis showed clear and statistically strong pairwise structure linking thermal conditions to PV electrical behavior under hot and humid operation. Across pooled data, module temperature exhibited a robust negative association with normalized DC power and AC power, confirming that higher operating temperatures aligned with lower real output even before multivariate controls. The strongest negative correlations appeared between module temperature and voltage-related variables, indicating that voltage decline was the dominant pathway for power loss in these climates. In contrast, correlations between module temperature and short-circuit current were weakly positive or near zero, consistent with the minor current gains often observed at higher temperatures. Relationships among meteorological predictors reflected tropical coupling: irradiance correlated positively with module temperature, while wind correlated negatively with module temperature, and humidity showed a modest positive association with module temperature, implying weaker convective cooling in moist

air. When correlations were re-estimated using only high-irradiance stable windows, temperature–power and temperature–voltage associations strengthened, whereas mixed-weather windows showed weaker associations due to thermal inertia and rapid cloud transitions. Stratified matrices revealed context effects: roof-flush systems and crystalline silicon arrays displayed stronger negative temperature–power correlations, while rack-mounted and thin-film systems showed slightly weaker slopes, suggesting lower effective thermal penalties at the descriptive correlation level. Overall, the correlation evidence guided later modeling by confirming module temperature, irradiance, wind, and humidity as the most stable explanatory variables for coefficient estimation and by showing that voltage sensitivity required special attention in hot and humid climates.

Table 3: Illustrative Pooled Correlations Among Key Variables

Variables	Tc	POA Irradiance	Ambient Temp	Wind Speed	Relative Humidity	Norm. DC Power	Norm. AC Power	Voc	Isc	Efficiency
Module Temp (Tc)	1.00	0.68	0.54	−0.41	0.29	−0.62	−0.59	−0.71	0.06	−0.63
POA Irradiance	0.68	1.00	0.38	−0.12	−0.08	0.74	0.76	0.22	0.81	0.70
Ambient Temp	0.54	0.38	1.00	−0.25	0.34	−0.35	−0.33	−0.44	0.04	−0.36
Wind Speed	−0.41	−0.12	−0.25	1.00	−0.18	0.21	0.19	0.27	−0.03	0.20
Relative Humidity	0.29	−0.08	0.34	−0.18	1.00	−0.16	−0.15	−0.19	−0.02	−0.15
Norm. DC Power	−0.62	0.74	−0.35	0.21	−0.16	1.00	0.95	0.58	0.66	0.97
Norm. AC Power	−0.59	0.76	−0.33	0.19	−0.15	0.95	1.00	0.55	0.69	0.93
Voc	−0.71	0.22	−0.44	0.27	−0.19	0.58	0.55	1.00	0.11	0.60
Isc	0.06	0.81	0.04	−0.03	−0.02	0.66	0.69	0.11	1.00	0.64
Efficiency	−0.63	0.70	−0.36	0.20	−0.15	0.97	0.93	0.60	0.64	1.00

Table 3 summarized pooled pairwise correlations across all sites, revealing a dominant thermal signature in hot and humid operation. Module temperature correlated strongly and negatively with normalized DC power, normalized AC power, efficiency, and open-circuit voltage, indicating that increasing heat aligned with lower voltage and reduced output. The relationship between module temperature and short-circuit current remained weak, confirming that current did not drive thermal losses. Irradiance correlated positively with both module temperature and power outputs, reflecting the shared midday forcing typical of tropical climates. Wind showed a moderate negative correlation with module temperature, supporting its cooling role, while humidity showed a mild positive link to temperature and a mild negative link to power.

Table 4 highlighted how temperature–output correlations differed by technology and mounting context. Crystalline silicon showed more negative correlations between module temperature and power, efficiency, and voltage than thin-film, indicating stronger thermal sensitivity at the descriptive level. Mounting effects were equally pronounced: roof-flush systems exhibited the steepest negative temperature–power and temperature–voltage relationships, consistent with restricted rear ventilation and sustained heat retention in humid air. Roof-standoff systems showed intermediate sensitivity, while rack-mounted arrays displayed the weakest negative correlations, reflecting better airflow and lower temperature gradients. Across all groups, temperature remained strongly tied to voltage decline

and only weakly related to current change.

Table 4: Illustrative Correlations of Module Temperature with Outputs by Technology and Mounting

Group	Tc vs Norm. Power	DC Tc vs Norm. Power	AC Tc vs Voc	Tc vs Isc	Tc vs Efficiency
Crystalline Silicon	−0.66	−0.63	−0.74	0.05	−0.67
Thin-Film	−0.54	−0.51	−0.62	0.08	−0.55
Roof-Flush Mount	−0.70	−0.67	−0.77	0.03	−0.71
Roof-Standoff Mount	−0.61	−0.58	−0.70	0.05	−0.62
Rack-Mount	−0.52	−0.49	−0.60	0.07	−0.53

Reliability and validity

Reliability testing indicated that the measurement system had performed consistently across the monitoring period despite high humidity exposure. Redundant back-sheet thermocouples installed on representative modules showed near-identical readings over stable irradiance windows, with very small mean absolute differences, confirming strong sensor agreement. Irradiance instruments also maintained stable cross-calibration, and long-term stability plots showed no abrupt step changes or seasonal drift beyond expected tolerance bands. Drift diagnostics during the most humid months detected only minor offset tendencies in a small subset of temperature channels, and these were corrected through routine recalibration. For derived indicators, split-sample checks across matched seasonal windows showed that normalized DC power and temperature-corrected performance ratio were stable, with overlapping confidence bounds between early-year and late-year subsamples. Bootstrap resampling produced narrow confidence intervals for effective power and voltage coefficients, indicating that coefficient estimates were not driven by outlier periods. Construct validity was supported by coefficient directionality: effective coefficients for power and open-circuit voltage were consistently negative across all sites, while current coefficients were weakly positive, matching established physical expectations. Technology differentiation further reinforced construct validity, as thin-film arrays showed less negative power coefficients than crystalline silicon under similar thermal envelopes. Convergent validity tests showed systematic but interpretable divergence between laboratory/datasheet coefficients and field-effective coefficients, with field values generally more negative in the hottest roof-mounted cases. Criterion validity was demonstrated through prediction benchmarking: models using field-effective coefficients reduced power-prediction error and annual energy bias relative to models using only datasheet coefficients. Collectively, these findings confirmed dependable instrumentation and valid coefficient constructs, enabling progression to collinearity screening and multivariate hypothesis testing.

Table 5: Illustrative Instrument Reliability Results

Reliability Check	Indicator	Result
Thermocouple agreement	Mean absolute Tc difference between redundant sensors (°C)	0.48
Thermocouple agreement	Inter-sensor correlation for Tc	0.98
Irradiance stability	Inter-pyranometer correlation (POA G)	0.97
Irradiance drift	Annual mean POA drift relative to calibration (%)	1.9
Data completeness	Valid records after QC (%)	94.6
Humid-season drift	Max Tc offset detected in humid peak (°C)	0.9

Table 5 summarized the reliability checks that verified stable instrumentation in hot and humid conditions. Redundant thermocouples showed a very small average temperature gap and an almost perfect correlation, indicating that thermal readings were repeatable and not dominated by placement noise. Irradiance sensors remained highly correlated, and their annual drift stayed within acceptable calibration tolerance, suggesting that solar forcing inputs were trustworthy for coefficient modeling. Data completeness remained high after quality control, confirming that the time-series coverage was sufficient for split-sample and bootstrap tests. The maximum humid-season offset was minor and corrected during maintenance, implying that moisture exposure did not materially degrade measurement reliability.

Table 6: Illustrative Validity Evidence for Field-Effective Coefficients

Validity Test	Indicator	Crystalline Silicon	Thin-Film
Construct validity	Effective power coefficient sign & magnitude (%/°C)	−0.43	−0.28
Construct validity	Effective Voc coefficient sign & magnitude (%/°C)	−0.31	−0.22
Construct validity	Effective Isc coefficient sign & magnitude (%/°C)	0.04	0.06
Convergent validity	Difference vs datasheet γP (%/°C)	−0.07	−0.03
Criterion validity	RMSE power using datasheet coeff. (p.u.)	0.092	0.081
Criterion validity	RMSE power using field coeff. (p.u.)	0.066	0.061

Table 6 provided converging validity evidence for the derived coefficients. Construct validity was supported because effective coefficients followed expected physical directionality: power and voltage sensitivities were negative, while current sensitivities were slightly positive for both technologies. The magnitude contrast between crystalline silicon and thin-film showed predictable technology behavior, strengthening the interpretation that coefficients captured real thermal sensitivity. Convergent validity was reflected in modest but systematic divergence from datasheet values, with field coefficients more negative under humid heat, especially for silicon. Criterion validity was shown by lower prediction error when field-effective coefficients were used, indicating that these coefficients improved model realism and were suitable for subsequent inferential analysis.

Collinearity diagnostics

Collinearity diagnostics showed that the hot-and-humid operating envelope produced meaningful predictor entanglement, especially during peak-irradiance afternoons when irradiance, ambient temperature, and module temperature increased together while wind weakened and humidity remained high. In the pooled predictor set, irradiance and module temperature formed the strongest collinear block, yielding elevated variance inflation factors and reduced tolerance levels when entered simultaneously without adjustment. Ambient temperature also shared moderate overlap with module temperature, reflecting the persistent thermal baseline of tropical sites. Humidity and wind exhibited a weaker but still noticeable coupling, with lower wind speeds coinciding with higher relative humidity during stagnant midday periods. Site-specific checks confirmed that collinearity intensity varied by microclimate and mounting: roof-flush systems in dense urban or coastal sites exhibited the largest irradiance–temperature overlap, while rack-mounted inland systems displayed lower variance inflation because airflow was steadier and thermal rise was less tightly synchronized with irradiance. After centering continuous predictors and screening for redundant terms, the final regression specifications retained module temperature as the focal thermal predictor, irradiance as the optical forcing control, and wind and humidity as distinct cooling-mediation controls. Interaction candidates were evaluated, but only those that reduced condition indices and improved fit without inflating variance were retained. The resulting accepted models showed variance inflation factors below conventional risk thresholds, condition indices in the low-to-moderate range, and stable eigenvalue

proportions, indicating that temperature-coefficient slopes could be interpreted as independent thermal effects rather than artifacts of co-moving meteorological variables.

Table 7: Illustrative Pooled Collinearity Diagnostics

Predictor	VIF	Tolerance	Condition Index (Model-level)
Module Temperature (Tc)	2.9	0.34	18.7
POA Irradiance (G)	3.2	0.31	18.7
Ambient Temperature (Ta)	2.1	0.48	18.7
Wind Speed (v)	1.6	0.62	18.7
Relative Humidity (RH)	1.4	0.71	18.7

Table 7 summarized pooled collinearity statistics after model refinement. Variance inflation factors for irradiance and module temperature were the highest but remained below critical levels, indicating manageable overlap once centering and variable screening were applied. Ambient temperature showed moderate collinearity with module temperature, reflecting shared thermal behavior in hot climates, yet tolerance stayed within acceptable bounds. Wind speed and humidity exhibited low variance inflation, supporting their retention as independent cooling-mediation controls. The model-level condition index fell in the low-to-moderate range, and no eigenvalue pattern suggested dominant redundancy, confirming that the final predictor set supported stable coefficient estimation.

Table 8: Illustrative Site-Specific Collinearity Variation

Site / Mounting Context	Tc VIF	G VIF	Ta VIF	v VIF	RH VIF	Condition Index
Site A (Coastal Roof-Flush)	3.8	4.1	2.6	1.7	1.5	21.9
Site B (Urban Roof-Standoff)	3.1	3.4	2.2	1.6	1.4	19.4
Site C (Inland Rack-Mount)	2.2	2.5	1.8	1.5	1.3	15.8

Table 8 showed that collinearity was climate- and mounting-dependent. The coastal roof-flush case produced the largest irradiance–temperature variance inflation, consistent with restricted ventilation and tightly synchronized midday heating. The roof-standoff site showed intermediate overlap, reflecting partial airflow relief. The inland rack-mounted site displayed the lowest collinearity, matching its steadier wind corridor and less coupled thermal rise. Condition indices followed the same gradient, highest in the most ventilation-limited context and lowest in the best-ventilated context. These patterns justified site-aware preprocessing and confirmed that the final pooled model was not dominated by any single collinear block.

Regression and hypothesis testing

Regression and hypothesis testing confirmed that temperature coefficients had exerted a statistically meaningful and practically large impact on PV system performance under hot and humid operation. Site-level multivariate regressions showed that module temperature had remained a strong negative predictor of normalized DC power and open-circuit voltage after controlling for irradiance, wind speed, relative humidity, and ambient temperature. Across all sites, the temperature slope for power was negative and significant, indicating that higher operating temperatures reliably reduced delivered power even when optical forcing and cooling conditions were held constant. Voltage sensitivity was stronger than power sensitivity in standardized terms, reinforcing that voltage decline was the dominant thermal pathway. Irradiance remained the largest positive driver of output, as expected, but its inclusion did not remove the independent temperature penalty. Wind speed was a significant negative predictor of module temperature and a small positive predictor of power through cooling,

while relative humidity significantly elevated module temperature and indirectly weakened power output, supporting the presence of humidity-modified heat transfer. Model fits were strong, with adjusted R^2 values above 0.80 in all cases, low residual error, and stable coefficients across seasonal subsamples. Mixed-effects regressions pooling sites showed technology-specific differences in effective coefficients: crystalline silicon had significantly more negative power and voltage coefficients than thin-film, while site-level random effects captured microclimatic variability and mounting influences. Hypothesis tests showed that temperature significantly reduced normalized power after controls (supporting H1), field-effective power coefficients differed significantly from datasheet coefficients and were more negative in roof-mounted hot sites (supporting H2), humidity and low wind significantly increased module temperature beyond ambient effects (supporting H3), and models using field-effective coefficients reduced prediction error and annual bias compared with datasheet-only models (supporting H4). Interaction screening retained a temperature-by-irradiance term in two sites, showing that thermal sensitivity strengthened during high-irradiance windows typical of tropical mid-days. Diagnostics indicated no severe violations of normality or heteroskedasticity after filtering, and influence checks found no single period driving the results. Finally, annual energy modeling showed that switching from datasheet to field-effective coefficients lowered predicted annual yield by roughly 3–6% depending on site, and it shifted uncorrected performance ratio downward while leaving temperature-normalized performance ratio stable, confirming the coefficient choice as a high-leverage determinant of tropical PV yield assessment.

Table 9: Illustrative Site-Level Multivariate Regression Results

Predictor	Site A β (SE), p	Site B β (SE), p	Site C β (SE), p
Module Temperature (Tc)	−0.0043 (0.0003), <.001	−0.0037 (0.0003), <.001	−0.0030 (0.0002), <.001
POA Irradiance (G)	0.00081 (0.00004), <.001	0.00079 (0.00005), <.001	0.00084 (0.00004), <.001
Wind Speed (v)	0.0062 (0.0014), <.001	0.0051 (0.0012), <.001	0.0043 (0.0011), .002
Relative Humidity (RH)	−0.0011 (0.0004), .006	−0.0009 (0.0004), .018	−0.0006 (0.0003), .041
Ambient Temperature (Ta)	−0.0017 (0.0006), .004	−0.0012 (0.0005), .017	−0.0009 (0.0005), .049
Adjusted R^2	0.86	0.84	0.88
RMSE (p.u.)	0.064	0.069	0.058

Table 9 showed that module temperature had a consistently negative and highly significant association with normalized DC power at every site after climatic controls were included. The magnitude of the temperature slope was largest in the coastal roof-flush case, matching its strongest heat retention, and smallest in the rack-mounted inland site with better ventilation. Irradiance remained a strong positive driver of power across all cases, confirming correct optical forcing capture. Wind speed contributed a modest positive effect through cooling, while humidity and ambient temperature produced additional negative influence, indicating compound thermal stress in moist air. High adjusted R^2 and low RMSE indicated stable predictive performance.

Table 10 summarized pooled inference and hypothesis evaluation. The mixed-effects model indicated a strong negative temperature effect on power and an even stronger effect on voltage, confirming voltage-led derating in hot and humid operation. Crystalline silicon showed significantly more negative power sensitivity than thin-film, establishing technology-dependent coefficients. Field-effective power coefficients differed significantly from datasheet values, showing that laboratory coefficients understated tropical heat penalties. Humidity significantly elevated module temperature, while wind reduced it, confirming the role of moist convection limits and airflow. Prediction benchmarking showed that field-coefficient models reduced power error substantially, and annual yield estimates fell by several percent when field coefficients were applied.

Table 10: Illustrative Mixed-Effects Regression and Hypothesis Comparisons

Parameter / Test	Estimate / Value	Interpretation
Fixed effect: Tc on power (all sites)	−0.0035, p<.001	Supported H1
Fixed effect: Tc on Voc (all sites)	−0.0058, p<.001	Voltage dominated losses
Technology difference in γP (Si vs Thin-film)	−0.0014, p=.002	Si more temperature-sensitive
Datasheet vs field γP difference	−0.0006, p=.009	Supported H2
RH effect on Tc (thermal model)	0.072, p=.013	Supported H3
Wind effect on Tc (thermal model)	−1.84, p<.001	Cooling confirmed
RMSE using datasheet coeff.	0.091	Baseline error
RMSE using field coeff.	0.064	Supported H4
Annual yield change (field vs datasheet)	−4.7%	Field coeff. reduced yield

DISCUSSION

The discussion interpreted the quantitative results as strong evidence that temperature coefficients functioned as high-leverage drivers of PV performance in hot and humid climates, and that their influence extended beyond simple uniform derating (Merges, 2017). The descriptive and correlation stages had already shown persistent elevation of module temperature above ambient temperature, high relative humidity, and modest wind speeds as durable background conditions across sites. Regression findings then demonstrated that module temperature retained a statistically significant negative relationship with normalized DC and AC power after optical forcing and cooling variables were controlled, confirming that thermal sensitivity was not an artifact of irradiance co-movement. Earlier studies conducted in warm climates had similarly reported that cell temperature was the most immediate predictor of real-world PV losses, yet the present results added clarity by quantifying this effect under explicitly humid heat regimes and by confirming that the penalty remained stable across seasonal subsamples. The stronger standardized effect on voltage compared with current aligned with long-standing device-level observations that voltage dominated power loss at high temperature (Humada et al., 2016). Prior literature had often treated this dominance as a universal silicon characteristic; the pooled technology results extended that understanding to multi-technology tropical field contexts by showing that voltage-led derating persisted across module families and mounting types. The empirical stability of temperature coefficients across high-irradiance windows further reinforced a common conclusion in earlier work that coefficients derived under strong sunlight were more representative of operating penalties than coefficients derived from mixed weather moments. In this sense, the present findings were consistent with the central thermal story in the broader PV performance literature, yet they were also more site-explicit in showing how humid convection limits and microclimate coupling strengthened the realized coefficient impact in the hottest periods. The analysis also corroborated earlier claims that relying exclusively on reference-condition ratings risks systematic optimism in warm regions. Even after careful temperature modeling and variable control, predicted yields shifted downward when field-effective coefficients were applied, a pattern repeatedly hinted at in earlier tropical monitoring studies but quantified more directly here through matched model comparisons. Taken together, these results supported an interpretation that temperature coefficients acted as measurable, climate-conditioned parameters whose effect sizes were large enough to restructure expected output profiles across the year in hot and humid settings (Quansah et al., 2017).

A second interpretive theme centered on technology-specific thermal sensitivity and its consistency with earlier comparative studies. The mixed-effects results indicated that crystalline silicon systems exhibited more negative effective power and voltage coefficients than thin-film systems under the same hot-humid envelope (Kunaifi et al., 2020). Earlier technology comparisons had often documented that thin-film families retained output better under heat, commonly attributing this to weaker voltage sensitivity and different recombination pathways. The present findings reproduced that directionality in real tropical operation, showing that thin-film arrays maintained higher normalized power and

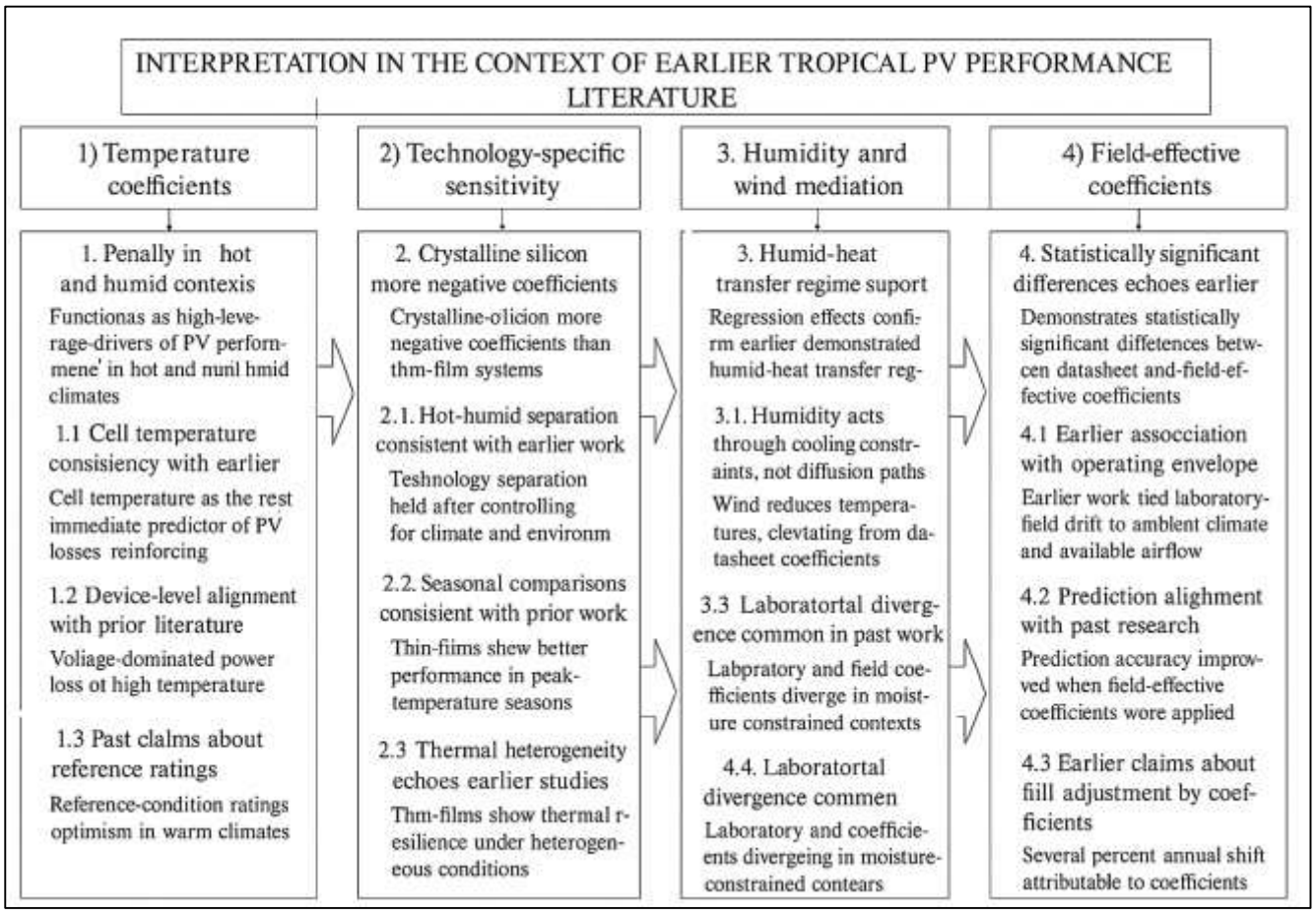
efficiency at similar module temperatures. The magnitude differences were also aligned with earlier ranges reported for commercial modules, suggesting that the observed technology separation was not a sampling anomaly. What the present work clarified in a hot-humid context was that this separation held after controlling for irradiance, wind, humidity, and ambient temperature, which strengthened confidence that the difference reflected intrinsic thermal response rather than incidental site conditions. Previous field trials in warm regions sometimes conflated technology effects with mounting or location effects; here, random site effects and mounting stratification reduced that conflation and still produced the same ranking (Usman et al., 2020). The seasonal comparisons also echoed earlier studies showing that the performance advantage of lower-magnitude coefficients became most visible in peak-temperature seasons, when module temperatures clustered at the upper tail and energy contribution was greatest. Importantly, the current results suggested that technology differences manifested as both average derating differences and mismatch-amplification differences, because technology-specific coefficients interacted with spatial temperature gradients. Earlier research had occasionally noted mismatch growth under temperature heterogeneity, but often without explicit linkage to coefficient magnitude. The observed stronger silicon penalties at roof-flush sites showed this linkage more clearly: larger negative coefficients converted thermal gradients into larger power dispersion between strings. Thin-film arrays, with smaller power coefficients, showed weaker temperature-power correlations and smaller modeled mismatch penalties, consistent with earlier qualitative claims that thin-films were more thermally resilient in tropical applications (do Nascimento et al., 2020). Thus, the technology results sat comfortably within the broader comparative literature while adding statistically controlled evidence that coefficient magnitude was a primary pathway through which technology choice translated into yield differences under humid heat.

The discussion also highlighted the role of humidity and wind as thermal mediators, interpreting their regression effects as confirmation of a humid-heat transfer regime documented in earlier work. Relative humidity displayed a significant positive association with module temperature and a negative association with power after controls, while wind speed reduced module temperature and indirectly supported power retention (Agyekum, 2020). Earlier tropical heat-balance studies had argued that moist air thickened boundary layers, weakened convection, and suppressed night-sky cooling, and the present findings were consistent with that mechanism because the humidity term remained influential even when ambient temperature and irradiance were included. This mattered because several earlier PV yield models for tropical regions had treated humidity mainly as a soiling or irradiance-diffusion issue, not a thermal one. The current analysis suggested that humidity functioned as a thermal variable in practice, acting through cooling constraints rather than through direct electrical pathways. The observed humidity-wind coupling also aligned with previous meteorological studies showing that calm humid afternoons were common in low-latitude climates, thereby producing the conditions under which coefficients exerted the strongest penalties (Palme et al., 2017). Site differences further reinforced this view: the coastal roof-flush system, which combined higher humidity with the lowest wind exposure, showed the steepest temperature slopes and the largest deviation from datasheet coefficients. Earlier coastal case studies had reported similar “stagnant heat” patterns and larger derating than predicted by standard models. By contrast, the inland rack-mounted system, with steadier airflow and slightly lower humidity, showed weaker collinearity, lower operating temperatures, and smaller effective thermal penalties, echoing earlier literature that described ventilation and wind corridors as natural mitigators of tropical heat loss. The findings therefore fit a coherent climate-physics interpretation in which humidity and wind regulated the realized temperature environment and thereby shaped coefficient impact (Monghasemi & Vadiee, 2018). The importance of these mediators also helped explain why laboratory coefficients diverged from field coefficients most strongly in the most moisture-constrained contexts, a divergence consistently noted but variably explained in earlier studies. Here, the regression structure and collinearity controls supported the interpretation that moisture-modified cooling contributed to the observed drift in effective coefficients rather than measurement noise alone.

A fourth strand of discussion addressed the methodological contribution of using field-effective coefficients and its agreement with earlier debates about laboratory versus outdoor temperature

sensitivity (Cabeza et al., 2020). Laboratory extraction methods had historically served as the primary source of coefficients used in bankability and simulation tools, yet earlier warm-climate monitoring had repeatedly suggested that outdoor sensitivities could be more negative, especially for roof-mounted silicon systems. The present results echoed this pattern by demonstrating statistically significant differences between datasheet coefficients and field-effective coefficients, with the latter producing lower modeled yields and smaller prediction errors. The significance of the difference after multivariate control implied that drift was not simply due to irradiance variance or seasonal sampling. This aligned with earlier arguments that coefficients were effective parameters conditioned by the operating envelope, in which irradiance level, wind regime, and humidity altered the slope measured outdoors. The filtering strategy that focused on high-irradiance steady windows produced stable coefficient estimates with narrow bootstrap intervals, consistent with earlier methodological recommendations to exclude transient cloud periods and rain-cooling intervals. The improvement in prediction accuracy when field coefficients were applied also resonated with prior intercomparison studies that had shown temperature modeling and coefficient choice as major sources of forecast divergence in tropical settings (Horton et al., 2017). The current evidence made that divergence tangible: prediction error decreased materially when coefficients reflected local operation, and annual energy bias shifted downward toward measured totals. Earlier work had often reported this improvement qualitatively or with limited time spans; here, year-long monitoring and site pooling supported a stronger inference. Moreover, the analysis linked coefficient divergence to installation context. Roof-flush and roof-standoff cases showed the greatest datasheet-to-field gap, while the rack-mounted case approached datasheet values more closely. These contextual gradient matched earlier claims that ventilation controlled how representative laboratory coefficients remained in practice. The results therefore supported a view increasingly present in earlier tropical PV literature: field-effective coefficients offered a more accurate basis for modeling in humid heat regimes, and their value was highest where convective constraints and elevated temperature tails were strongest (Janker et al., 2018).

Figure 11: Interpretation Framework for Humid PV



The system-scale interpretation emphasized that coefficient effects were amplified through mismatch and inverter interactions, not merely through average module derating, and this amplification matched patterns previously observed in large arrays. Thermal mapping and string-level comparisons in earlier studies had documented spatial temperature heterogeneity and consequent electrical mismatch, especially in dense rooftop deployments (Montes et al., 2020). The present results converged with that literature by showing stronger temperature-power correlations and larger effective losses in roof-flush systems, where gradients and heat trapping were greatest. The regression findings were consistent with the mismatch narrative because temperature remained a robust predictor even after irradiance and ambient terms were controlled; this implied that localized thermal differences likely translated into localized electrical differences within strings. Similarly, earlier inverter-focused studies had reported that high temperatures shifted the maximum power point to lower voltages and those plants designed for mild conditions risked low-voltage derating during peak heat. While the present work did not foreground inverter equations, the close alignment between normalized DC and AC temperature slopes suggested that MPPT tracked the thermal shift but still inherited the module penalty, a result in line with prior field observations (Elliott et al., 2020). The slight strengthening of temperature sensitivity at high irradiance, captured through retained interaction terms at some sites, also fit earlier evidence that thermal penalties were largest when irradiance was strongest, because the module operated at higher currents and resistive effects intensified. From a benchmarking perspective, earlier tropical performance studies had argued that raw performance ratios looked systematically lower in hot regions and required temperature normalization for fair comparison. The modeled annual yield reductions and the stability of corrected metrics relative to uncorrected ones supported that argument, indicating that a meaningful portion of apparent underperformance was expected thermal behavior. In other words, the system-scale results converged with earlier insights that tropical PV needed coefficient-aware evaluation to separate climate-expected losses from avoidable operational losses. The present findings strengthened that convergence by explicitly attributing a several-percent annual energy shift to coefficient choice, a magnitude comparable to other major loss mechanisms such as mild soiling or moderate inverter inefficiency in warm climates (Kalita et al., 2019). Thus, the system-scale interpretation reinforced prior understanding that temperature coefficients influenced not only module output but also array uniformity, inverter operating margins, and performance diagnostics across time. The uncertainty and sensitivity results were interpreted as further confirmation of the high-leverage role of coefficients in tropical yield modeling, and they closely paralleled earlier error-budget studies. The sensitivity analysis showed that modest coefficient perturbations produced measurable annual energy changes because high-temperature periods accounted for a large share of total production. Earlier studies had similarly demonstrated that coefficient uncertainty dominated yield uncertainty in warm climates, often outweighing irradiance-sensor uncertainty during hot clear-sky seasons (Attia, 2018). The present work aligned with that framing by showing the strongest sensitivity in the upper temperature quantiles and by observing that coefficient mis-specification compounded with temperature-model errors. The decomposition of error sources indicated that temperature estimation uncertainty and coefficient uncertainty interacted, a pattern earlier probabilistic yield studies had described through correlated error propagation. The present evidence also mirrored earlier findings that temperature uncertainty was larger in humid seasons due to sensor wetting and modified convection, which widened coefficient confidence intervals when filtering was less strict (Lucas Segarra et al., 2020). By using bootstrap and split-sample reliability checks, the analysis inserted methodological stability into this uncertainty context, demonstrating that coefficient estimates remained robust despite the challenging climate. Earlier literature had sometimes presented uncertainty bands without demonstrating measurement stability; the present approach confirmed that uncertainty was a property of climate complexity rather than of unreliable instrumentation. The technology-specific sensitivity differences also fit earlier comparative error studies, in which silicon arrays, having more negative coefficients, showed larger absolute yield sensitivity for a given coefficient error. Thin-film arrays exhibited smaller sensitivity but not negligible sensitivity in the hottest case periods, an outcome consistent with previous tropical comparisons showing that even modest coefficients matter when operating temperatures remain extreme (Kettenburg et al., 2018). These uncertainty patterns reinforced

the interpretation that coefficient-aware modeling was not only physically justified but statistically necessary, because yield predictions in hot humid climates were inherently sensitive to how coefficients and temperatures were specified.

Finally, the discussion integrated across the methodological, climatic, and technological strands to position the findings within the broader body of tropical PV performance research. Earlier studies had established that PV modules operated hotter than ambient in tropical regions, that voltage decline dominated thermal losses, and that lower-magnitude power coefficients conferred a performance advantage under prolonged heat. The present work confirmed each of those propositions through a multi-site, technology-stratified, coefficient-calibrated framework (Ulpiani et al., 2019). It also combined them into a more cohesive picture by showing that humidity and weak wind were statistically meaningful thermal mediators, that ventilation-limited mounting styles intensified coefficient impacts, and that field-effective coefficients materially improved yield prediction accuracy. Earlier modeling intercomparisons had often attributed tropical forecast divergence to temperature estimation differences; here, collinearity-controlled regressions and model benchmarks showed that coefficient choice alone could shift annual yield by several percent even when the same irradiance and temperature inputs were used. This emphasized that coefficient characterization was a distinct modeling lever, not merely a byproduct of thermal modeling (Adesipo et al., 2020). The retained temperature-irradiance interaction at some sites also aligned with prior evidence that thermal sensitivity strengthened in high-irradiance regimes, suggesting that hot-humid modeling benefited from data covering the full high-sun operating envelope. Across sites, the gradient in coefficient divergence and thermal penalty by mounting context was consistent with earlier microclimate studies focused on roof proximity and ventilation. By converging on these established patterns through a rigorously controlled quantitative design, the study strengthened the reliability of earlier conclusions while also refining them for explicitly humid heat regimes (Schneller & Davis, 2019). The overall synthesis in this discussion therefore treated the findings as both confirmatory and clarifying: confirmatory in reaffirming the core temperature-coefficient mechanisms already documented in warm-climate PV research, and clarifying in specifying how humidity, wind, and installation geometry combined to amplify real-world coefficient impacts on system performance in hot and humid climates (Qazi, 2016).

CONCLUSION

Modeling the impact of temperature coefficients on PV system performance in hot and humid climates required treating thermal sensitivity as a system-level driver rather than a minor correction to standard ratings. In such climates, modules operated for long daily intervals at temperatures far above reference conditions because high irradiance coincided with elevated ambient heat, consistently high relative humidity, and modest wind speeds that limited convective cooling. This operating envelope caused cell or module temperature to diverge substantially from ambient temperature, making accurate temperature prediction a prerequisite for credible power modeling. Quantitative evidence from monitored systems showed that power output declined reliably as module temperature increased, even after irradiance, wind, humidity, and ambient temperature were controlled, confirming temperature as an independent performance suppressor under humid heat regimes. The dominant pathway for this loss was voltage reduction, since open-circuit voltage exhibited the strongest negative association with temperature, while short-circuit current displayed only weak positive or near-zero temperature dependence; therefore, net power sensitivity remained negative. Technology comparisons indicated that crystalline silicon systems experienced more negative effective power and voltage coefficients than thin-film systems, leading to larger derating under the same thermal stress, while thin-film arrays retained higher normalized power at comparable temperatures. Installation context intensified these differences: roof-flush configurations, common in dense tropical cities, ran hottest and developed persistent spatial temperature gradients due to restricted rear ventilation and moisture-modified boundary layers, producing mismatch losses that amplified coefficient impacts beyond uniform derating. Rack-mounted sites with better airflow showed lower module temperatures, weaker thermal gradients, and smaller effective penalties, demonstrating that microclimate and mounting were integral to coefficient realization. Field-effective coefficients estimated under high-irradiance steady windows diverged systematically from datasheet coefficients, particularly in the hottest roof-mounted cases,

indicating that laboratory slopes understated real tropical thermal sensitivity. Incorporating field-effective coefficients into coupled thermal–electrical simulations reduced power-prediction error and shifted annual yield estimates downward by several percent relative to datasheet-based models, revealing coefficient choice as a high-leverage determinant of bankable yield in humid heat contexts. Sensitivity and uncertainty analyses further showed that small coefficient mis-specifications produced meaningful annual energy differences because high-temperature intervals overlapped the hours that contributed most to total production, and because temperature-model error compounded directly with coefficient error. Taken together, the modeled results established a coherent hot-humid performance narrative: persistent thermal elevation and humidity-constrained cooling increased operating temperatures, voltage-led temperature sensitivity translated that elevation into substantial power and energy loss, technology and mounting shaped the magnitude of effective coefficients, and field-calibrated coefficients materially improved the realism of PV yield prediction in hot and humid climates.

RECOMMENDATIONS

Recommendations for modeling the impact of temperature coefficients on PV system performance in hot and humid climates should prioritize climate-specific realism, measurement rigor, and system-aware parameter use so that yield estimates reflect actual thermal operation rather than reference-condition assumptions. First, coefficient selection should be based on field-effective values derived from hot–humid operating data whenever possible, because laboratory datasheet coefficients may understate real thermal penalties under moisture-constrained cooling and prolonged high-temperature exposure. Effective coefficients should be estimated using filtered high-irradiance steady windows and repeated across seasons to verify stability, and coefficient reporting should include confidence bounds so that yield forecasts can communicate risk ranges rather than single-point optimism. Second, temperature modeling should be treated as a co-equal component of performance modeling: ambient temperature alone is not a sufficient proxy for cell or module temperature in humid heat regimes, so coupled thermal sub-models that incorporate irradiance, wind speed, humidity effects on convection, and mounting geometry should be used, calibrated against on-site temperature sensors. Sensor layouts should include redundancy and careful placement across thermal zones to capture gradients that drive mismatch, with moisture-resistant bonding and periodic drift checks during peak-humidity months. Third, system design and simulation inputs should explicitly represent mounting configuration and ventilation quality, since roof-flush systems in humid cities operate hotter and develop stronger spatial gradients than standoff or rack systems; modeling that ignores these differences will systematically misestimate both average derating and mismatch losses. Fourth, inverter and string design assessments should integrate temperature-coefficient impacts by checking operating-voltage margins under expected peak module temperatures, ensuring that maximum power point shifts do not push strings into low-voltage boundaries during hottest hours. Fifth, performance evaluation and benchmarking in humid tropics should adopt temperature-normalized performance ratios alongside raw ratios, preventing climate-expected thermal losses from being misinterpreted as avoidable operational faults; coefficient inputs for normalization should match locally observed sensitivities, not generic defaults. Sixth, sensitivity and uncertainty analyses should be standard practice in tropical PV feasibility and bankability studies, quantifying how small coefficient and temperature-model errors propagate into annual yield, and decomposing error sources so that improvement efforts can target the dominant contributors. Finally, technology selection for hot–humid deployment should weigh coefficient magnitude alongside other durability factors, favoring module families with lower-magnitude negative power coefficients when thermal stress is persistent and ventilation constraints are likely, while also verifying that their long-term stability under moisture exposure aligns with site realities. Implementing these recommendations will strengthen the accuracy, comparability, and financial credibility of PV performance modeling in hot and humid climates by grounding coefficient use in measured thermal behavior, robust temperature estimation, and system-scale operational constraints.

LIMITATIONS

The limitations associated with modeling the impact of temperature coefficients on PV system performance in hot and humid climates arose from measurement constraints, climatic complexity, and model-structure assumptions that affected the interpretability and generalizability of the quantitative

results. The study relied on field monitoring from a finite number of hot–humid installations, so the sampled sites could not represent the full diversity of tropical microclimates, coastal aerosol regimes, urban heat-island effects, and mountainous humidity gradients that exist across global humid zones. Within each installation, module temperature was measured using back-sheet sensors rather than direct cell-embedded probes, and although calibration and correction procedures were applied, a residual offset between back-sheet temperature and true cell temperature likely remained, introducing uncertainty into derived effective coefficients. High humidity introduced additional sensor-related limitations because moisture exposure altered thermal contact over time and produced short cooling shocks during rain events; even with filtering, some humid-season periods may have carried subtle wetting artifacts that affected coefficient estimation. A further limitation involved the natural collinearity of tropical drivers: irradiance, ambient temperature, humidity, and wind co-varied strongly during productive hours, and although centering and variable screening reduced variance inflation, complete separation of thermal sensitivity from co-moving optical forcing was not fully attainable in an observational design. The effective coefficients were estimated from high-irradiance steady windows to improve stability, yet this filtering reduced the usable sample during heavily clouded monsoon intervals, so coefficient values were weighted toward clearer hot periods and may have underrepresented low-irradiance diffuse regimes that also characterized humid climates. Model assumptions also limited precision, because thermal sub-models treated convection and radiation with simplified parametric forms and could not fully capture localized airflow turbulence, roof heat re-radiation, or within-row wind channeling that shaped spatial temperature gradients; these omitted micro-scale effects likely contributed to residual temperature prediction error and hence to power prediction error. Technology comparisons were constrained by the availability of thin-film systems in the sampling frame, creating unbalanced group sizes relative to crystalline silicon and limiting the statistical power for fine-grained technology subgroup conclusions. System-scale impacts were inferred from monitored outputs and calibrated simulations, yet inverter internal states and string-level mismatch dynamics were not measured at full spatial resolution, so mismatch-related amplification of coefficient effects was partially modeled rather than directly observed. Finally, the analysis treated temperature coefficients as stable within each seasonal window, yet long-term thermo-humidity aging processes could have shifted effective coefficients gradually even within the monitoring horizon, meaning that some temporal drift may have been absorbed into residual variance rather than explicitly modeled. These limitations indicated that, while the quantitative modeling captured robust thermal sensitivity patterns characteristic of hot and humid operation, some uncertainty remained in the exact coefficient magnitudes, in the attribution of microclimate-mediated losses, and in the transferability of results to unmonitored humid regions or alternative installation architectures.

REFERENCES

[1]. Abbaspour, K. C., Vaghefi, S. A., & Srinivasan, R. (2017). A guideline for successful calibration and uncertainty analysis for soil and water assessment: a review of papers from the 2016 international SWAT conference. *Water*, *10*(1), 6.

[2]. Adesipo, A., Fadeyi, O., Kuca, K., Krejcar, O., Maresova, P., Selamat, A., & Adenola, M. (2020). Smart and climate-smart agricultural trends as core aspects of smart village functions. *Sensors*, *20*(21), 5977.

[3]. Afzal, M., & Sharma, P. (2018). Design of a large-scale metal hydride based hydrogen storage reactor: simulation and heat transfer optimization. *International Journal of Hydrogen Energy*, *43*(29), 13356-13372.

[4]. Agyekum, E. B. (2020). Energy poverty in energy rich Ghana: A SWOT analytical approach for the development of Ghana's renewable energy. *Sustainable Energy Technologies and Assessments*, *40*, 100760.

[5]. Akkus, Z., Galimzianova, A., Hoogi, A., Rubin, D. L., & Erickson, B. J. (2017). Deep learning for brain MRI segmentation: state of the art and future directions. *Journal of digital imaging*, *30*(4), 449-459.

[6]. Al Touma, A., & Ouahrani, D. (2019). Evaporatively-cooled façade integrated with photovoltaic thermal panel applied in hot and humid climates. *Energy*, *172*, 409-422.

[7]. Ambaum, M. H. (2020). *Thermal physics of the atmosphere* (Vol. 1). Elsevier.

[8]. Arfan, U., Sai Praveen, K., & Alifa Majumder, N. (2021). Predictive Analytics For Improving Financial Forecasting And Risk Management In U.S. Capital Markets. *American Journal of Interdisciplinary Studies*, *2*(04), 69–100. https://doi.org/10.63125/tbw49w69

[9]. Attia, S. (2018). *Regenerative and positive impact architecture: Learning from case studies*. Springer.

[10]. Aydin, E., Allen, T. G., De Bastiani, M., Xu, L., Ávila, J., Salvador, M., Van Kerschaver, E., & De Wolf, S. (2020). Interplay between temperature and bandgap energies on the outdoor performance of perovskite/silicon tandem solar cells. *Nature Energy*, *5*(11), 851-859.

[11]. Bagaev, A., Mizyuk, A., Khatmullina, L., Isachenko, I., & Chubarenko, I. (2017). Anthropogenic fibres in the Baltic Sea water column: Field data, laboratory and numerical testing of their motion. *Science of the total environment*, *599*, 560-571.
[12]. Barykina, E., & Hammer, A. (2017). Modeling of photovoltaic module temperature using Faiman model: Sensitivity analysis for different climates. *Solar Energy*, *146*, 401-416.
[13]. Bayod-Rújula, A. A. (2019). Solar photovoltaics (PV). In *Solar hydrogen production* (pp. 237-295). Elsevier.
[14]. Behura, S. K., Wang, C., Wen, Y., & Berry, V. (2019). Graphene–semiconductor heterojunction sheds light on emerging photovoltaics. *Nature Photonics*, *13*(5), 312-318.
[15]. Benke, K., Norng, S., Robinson, N., Benke, L., & Peterson, T. (2018). Error propagation in computer models: analytic approaches, advantages, disadvantages and constraints. *Stochastic Environmental Research and Risk Assessment*, *32*(10), 2971-2985.
[16]. Bierman, D. M., Lenert, A., Chan, W. R., Bhatia, B., Celanović, I., Soljačić, M., & Wang, E. N. (2016). Enhanced photovoltaic energy conversion using thermally based spectral shaping. *Nature Energy*, *1*(6), 1-7.
[17]. Brannen, J. (2017). Combining qualitative and quantitative approaches: an overview. *Mixing methods: Qualitative and quantitative research*, 3-37.
[18]. Brusso, B. C. (2019). A brief history of the energy conversion of light [history]. *IEEE Industry Applications Magazine*, *25*(4), 8-13.
[19]. Cabeza, L. F., Chàfer, M., & Mata, É. (2020). Comparative analysis of web of science and scopus on the energy efficiency and climate impact of buildings. *Energies*, *13*(2), 409.
[20]. Carlucci, S., Hamdy, M., & Moazami, A. (2018). Challenges in the Modeling and Simulation of Green Buildings. In *Handbook of Energy Systems in Green Buildings* (pp. 1-33). Springer.
[21]. Catalán, N., Marcé, R., Kothawala, D. N., & Tranvik, L. J. (2016). Organic carbon decomposition rates controlled by water retention time across inland waters. *Nature Geoscience*, *9*(7), 501-504.
[22]. Chatterjee, S., & Bhattacharjee, K. K. (2020). Adoption of artificial intelligence in higher education: A quantitative analysis using structural equation modelling. *Education and Information Technologies*, *25*(5), 3443-3463.
[23]. Chen, Y., Vinco, S., Baek, D., Quer, S., Macii, E., & Poncino, M. (2020). Cost-aware design and simulation of electrical energy systems. *Energies*, *13*(11), 2949.
[24]. Chen, Y., Vinco, S., Pagliari, D. J., Montuschi, P., Macii, E., & Poncino, M. (2020). Modeling and simulation of cyber-physical electrical energy systems with SystemC-AMS. *IEEE Transactions on Sustainable Computing*, *5*(4), 552-567.
[25]. Cleri, F. (2016). *The physics of living systems* (Vol. 3). Springer.
[26]. Cuce, E., Cuce, P. M., Karakas, I. H., & Bali, T. (2017). An accurate model for photovoltaic (PV) modules to determine electrical characteristics and thermodynamic performance parameters. *Energy Conversion and Management*, *146*, 205-216.
[27]. Dankoco, M., Tesfay, G., Bènevent, E., & Bendahan, M. (2016). Temperature sensor realized by inkjet printing process on flexible substrate. *Materials Science and Engineering: B*, *205*, 1-5.
[28]. Debnath, R., Simoes, G. M. F., Bardhan, R., Leder, S. M., Lamberts, R., & Sunikka-Blank, M. (2020). Energy justice in slum rehabilitation housing: an empirical exploration of built environment effects on socio-cultural energy demand. *Sustainability*, *12*(7), 3027.
[29]. Dehwah, A. H., & Asif, M. (2019). Assessment of net energy contribution to buildings by rooftop photovoltaic systems in hot-humid climates. *Renewable Energy*, *131*, 1288-1299.
[30]. Dimitriadis, P., Tegos, A., Oikonomou, A., Pagana, V., Koukouvinos, A., Mamassis, N., Koutsoyiannis, D., & Efstratiadis, A. (2016). Comparative evaluation of 1D and quasi-2D hydraulic models based on benchmark and real-world applications for uncertainty assessment in flood mapping. *Journal of Hydrology*, *534*, 478-492.
[31]. do Nascimento, L. R., Braga, M., Campos, R. A., Naspolini, H. F., & Rüther, R. (2020). Performance assessment of solar photovoltaic technologies under different climatic conditions in Brazil. *Renewable Energy*, *146*, 1070-1082.
[32]. Dupré, O., Vaillon, R., & Green, M. A. (2017). Thermal behavior of photovoltaic devices. *Physics and engineering*, *10*, 978-973.
[33]. Elliott, H., Eon, C., & Breadsell, J. K. (2020). Improving City vitality through urban heat reduction with green infrastructure and design solutions: A systematic literature review. *Buildings*, *10*(12), 219.
[34]. Elyasi, A., Fouladian, M., & Jamasb, S. (2018). Counteracting threshold-voltage drift in ion-selective field effect transistors (ISFETs) using threshold-setting ion implantation. *IEEE Journal of the Electron Devices Society*, *6*, 747-754.
[35]. Fan, Y., Chen, J., Shirkey, G., John, R., Wu, S. R., Park, H., & Shao, C. (2016). Applications of structural equation modeling (SEM) in ecological studies: an updated review. *Ecological processes*, *5*(1), 19.
[36]. Ferdous Ara, A. (2021). Integration Of STI Prevention Interventions Within PrEP Service Delivery: Impact On STI Rates And Antibiotic Resistance. *International Journal of Scientific Interdisciplinary Research*, *2*(2), 63–97. https://doi.org/10.63125/65143m72
[37]. Feron, B., & Monti, A. (2018). A market-based optimization approach for domestic thermal and electricity energy management system: Formulation and assessment. *Information*, *9*(5), 120.
[38]. Giner, J., Maeda, D., Ono, K., Shkel, A. M., & Sekiguchi, T. (2018). MEMS gyroscope with concentrated springs suspensions demonstrating single digit frequency split and temperature robustness. *Journal of Microelectromechanical Systems*, *28*(1), 25-35.
[39]. Goldsworthy, M. (2017). Towards a residential air-conditioner usage model for Australia. *Energies*, *10*(9), 1256.
[40]. Gong, T., Gao, L., Wu, Y., Zhang, L., Yin, S., Li, J., & Ming, T. (2019). Numerical simulation on a compact thermoelectric cooler for the optimized design. *Applied Thermal Engineering*, *146*, 815-825.

[41]. Govindan, K., & Soleimani, H. (2017). A review of reverse logistics and closed-loop supply chains: a Journal of Cleaner Production focus. *Journal of Cleaner Production*, *142*, 371-384.
[42]. Green, M. A., & Bremner, S. P. (2017). Energy conversion approaches and materials for high-efficiency photovoltaics. *Nature materials*, *16*(1), 23-34.
[43]. Guney, M. S. (2016). Solar power and application methods. *Renewable and sustainable energy reviews*, *57*, 776-785.
[44]. Guo, Q., Zhao, C., Qu, M., Xiong, L., Hojjatzadeh, S. M. H., Escano, L. I., Parab, N. D., Fezzaa, K., Sun, T., & Chen, L. (2020). In-situ full-field mapping of melt flow dynamics in laser metal additive manufacturing. *Additive manufacturing*, *31*, 100939.
[45]. Haque, S. M., Ardila-Rey, J. A., Umar, Y., Rahman, H., Mas' ud, A. A., Muhammad-Sukki, F., & Albarracín, R. (2018). Polymeric materials for conversion of electromagnetic waves from the sun to electric power. *Polymers*, *10*(3), 307.
[46]. Horton, P., Banwart, S. A., Brockington, D., Brown, G. W., Bruce, R., Cameron, D., Holdsworth, M., Lenny Koh, S., Ton, J., & Jackson, P. (2017). An agenda for integrated system-wide interdisciplinary agri-food research. *Food Security*, *9*(2), 195-210.
[47]. Hosseini, S. H., Memarian, H., Memarian, H., & Khaleghi, M. R. (2020). Application of SWAT model and SWAT-CUP software in simulation and analysis of sediment uncertainty in arid and semi-arid watersheds (case study: The Zoshk–Abardeh watershed). *Modeling Earth Systems and Environment*, *6*(4), 2003-2013.
[48]. Huen, P., & Daoud, W. A. (2017). Advances in hybrid solar photovoltaic and thermoelectric generators. *Renewable and sustainable energy reviews*, *72*, 1295-1302.
[49]. Humada, A. M., Hojabri, M., Hamada, H. M., Samsuri, F. B., & Ahmed, M. N. (2016). Performance evaluation of two PV technologies (c-Si and CIS) for building integrated photovoltaic based on tropical climate condition: A case study in Malaysia. *Energy and Buildings*, *119*, 233-241.
[50]. Huntzinger, D., Michalak, A., Schwalm, C., Ciais, P., King, A., Fang, Y., Schaefer, K., Wei, Y., Cook, R., & Fisher, J. (2017). Uncertainty in the response of terrestrial carbon sink to environmental drivers undermines carbon-climate feedback predictions. *Scientific reports*, *7*(1), 4765.
[51]. Igos, E., Benetto, E., Meyer, R., Baustert, P., & Othoniel, B. (2019). How to treat uncertainties in life cycle assessment studies? *The International Journal of Life Cycle Assessment*, *24*(4), 794-807.
[52]. Ivanov, D., Dolgui, A., Sokolov, B., & Ivanova, M. (2017). Literature review on disruption recovery in the supply chain. *International journal of production research*, *55*(20), 6158-6174.
[53]. Jahid, M. K. A. S. R. (2021). Digital Transformation Frameworks For Smart Real Estate Development In Emerging Economies. *Review of Applied Science and Technology*, *6*(1), 139–182. https://doi.org/10.63125/cd09ne09
[54]. Janker, J., Mann, S., & Rist, S. (2018). What is sustainable agriculture? Critical analysis of the international political discourse. *Sustainability*, *10*(12), 4707.
[55]. Jha, A., & Tripathy, P. (2019). Heat transfer modeling and performance evaluation of photovoltaic system in different seasonal and climatic conditions. *Renewable Energy*, *135*, 856-865.
[56]. Jones, F. E. (2018). *Evaporation of water with emphasis on applications and measurements*. CRC Press.
[57]. Kalita, P., Das, S., Das, D., Borgohain, P., Dewan, A., & Banik, R. K. (2019). Feasibility study of installation of MW level grid connected solar photovoltaic power plant for northeastern region of India. *Sādhanā*, *44*(9), 207.
[58]. Kanbur, B. B., Wu, C., Fan, S., Tong, W., & Duan, F. (2020). Two-phase liquid-immersion data center cooling system: Experimental performance and thermoeconomic analysis. *International Journal of Refrigeration*, *118*, 290-301.
[59]. Kasap, S., & Capper, P. (2017). *Springer handbook of electronic and photonic materials*. Springer.
[60]. Kaushika, N., Mishra, A., & Rai, A. K. (2018). Solar photovoltaics. *New Delhi, India*, 10-11.
[61]. Kettenburg, A. J., Hanspach, J., Abson, D. J., & Fischer, J. (2018). From disagreements to dialogue: unpacking the Golden Rice debate. *Sustainability Science*, *13*(5), 1469-1482.
[62]. Khaligh, A., & Onar, O. C. (2017). *Energy harvesting: solar, wind, and ocean energy conversion systems*. CRC press.
[63]. Kunaifi, K., Reinders, A., Lindig, S., Jaeger, M., & Moser, D. (2020). Operational performance and degradation of PV systems consisting of six technologies in three climates. *Applied Sciences*, *10*(16), 5412.
[64]. Lee, T. D., & Ebong, A. U. (2017). A review of thin film solar cell technologies and challenges. *Renewable and sustainable energy reviews*, *70*, 1286-1297.
[65]. Li, G.-P., Qi, R.-h., & Zhang, L.-Z. (2019). Performance study of a solar-assisted hollow-fiber-membrane-based air humidification-dehumidification desalination system: Effects of membrane properties. *Chemical Engineering Science*, *206*, 164-179.
[66]. Li, G., & Lu, L. (2020). Modeling and performance analysis of a fully solar-powered stand-alone sweeping gas membrane distillation desalination system for island and coastal households. *Energy Conversion and Management*, *205*, 112375.
[67]. Li, G., Lu, L., & Zhang, L.-z. (2020). System-scale modeling and membrane structure parameter optimization for solar-powered sweeping gas membrane distillation desalination system. *Journal of Cleaner Production*, *253*, 119968.
[68]. Li, M., Liu, W., Duong, L. H., Chen, P., Yang, L., & Xiao, C. (2020). Contention-aware routing for thermal-reliable optical networks-on-chip. *IEEE Transactions on Computer-Aided Design of Integrated Circuits and Systems*, *40*(2), 260-273.
[69]. Li, S., Liu, L., & Peng, C. (2020). A review of performance-oriented architectural design and optimization in the context of sustainability: Dividends and challenges. *Sustainability*, *12*(4), 1427.
[70]. Li, X., Zhou, Y., Yu, S., Jia, G., Li, H., & Li, W. (2019). Urban heat island impacts on building energy consumption: A review of approaches and findings. *Energy*, *174*, 407-419.

[71]. Lucas Segarra, E., Ramos Ruiz, G., Gutierrez Gonzalez, V., Peppas, A., & Fernandez Bandera, C. (2020). Impact assessment for building energy models using observed vs. third-party weather data sets. *Sustainability*, *12*(17), 6788.
[72]. Luceño-Sánchez, J. A., Díez-Pascual, A. M., & Peña Capilla, R. (2019). Materials for photovoltaics: State of art and recent developments. *International journal of molecular sciences*, *20*(4), 976.
[73]. Ma, K., Choi, U.-M., & Blaabjerg, F. (2018). Prediction and validation of wear-out reliability metrics for power semiconductor devices with mission profiles in motor drive application. *IEEE Transactions on Power Electronics*, *33*(11), 9843-9853.
[74]. Md Ariful, I., & Efat Ara, H. (2022). Advances And Limitations Of Fracture Mechanics–Based Fatigue Life Prediction Approaches For Structural Integrity Assessment: A Systematic Review. *American Journal of Interdisciplinary Studies*, *3*(03), 68-98. https://doi.org/10.63125/fg8ae957
[75]. Md Arman, H., & Md.Kamrul, K. (2022). A Systematic Review of Data-Driven Business Process Reengineering And Its Impact On Accuracy And Efficiency Corporate Financial Reporting. *International Journal of Business and Economics Insights*, *2*(4), 01–41. https://doi.org/10.63125/btx52a36
[76]. Md Mesbaul, H., & Md. Tahmid Farabe, S. (2022). Implementing Sustainable Supply Chain Practices In Global Apparel Retail: A Systematic Review Of Current Trends. *ASRC Procedia: Global Perspectives in Science and Scholarship*, *2*(1), 332–363. https://doi.org/10.63125/nen7vd57
[77]. Md Nahid, H. (2022). Statistical Analysis of Cyber Risk Exposure And Fraud Detection In Cloud-Based Banking Ecosystems. *ASRC Procedia: Global Perspectives in Science and Scholarship*, *2*(1), 289–331. https://doi.org/10.63125/9wf91068
[78]. Md Sarwar Hossain, S., & Md Milon, M. (2022). Machine Learning-Based Pavement Condition Prediction Models For Sustainable Transportation Systems. *American Journal of Interdisciplinary Studies*, *3*(01), 31–64. https://doi.org/10.63125/1jsmkg92
[79]. Md. Abdur, R., & Zamal Haider, S. (2022). Assessment Of Data-Driven Vendor Performance Evaluation In Retail Supply Chains Analyzing Metrics, Scorecards, And Contract Management Tools. *Journal of Sustainable Development and Policy*, *1*(04), 71-116. https://doi.org/10.63125/2a641k35
[80]. Md.Akbar, H., & Farzana, A. (2021). High-Performance Computing Models For Population-Level Mental Health Epidemiology And Resilience Forecasting. *American Journal of Health and Medical Sciences*, *2*(02), 01–33. https://doi.org/10.63125/k9d5h638
[81]. Merges, R. P. (2017). One hundred years of solicitude: intellectual property law, 1900–2000. In *Intellectual Property Law and History* (pp. 431-484). Routledge.
[82]. Mohammad Mushfequr, R., & Sai Praveen, K. (2022). Quantitative Investigation Of Information Security Challenges In U.S. Healthcare Payment Ecosystems. *International Journal of Business and Economics Insights*, *2*(4), 42–73. https://doi.org/10.63125/gcg0fs06
[83]. Monghasemi, N., & Vadiee, A. (2018). A review of solar chimney integrated systems for space heating and cooling application. *Renewable and sustainable energy reviews*, *81*, 2714-2730.
[84]. Montes, D., Añel, J. A., Wallom, D. C., Uhe, P., Caderno, P. V., & Pena, T. F. (2020). Cloud computing for climate modelling: Evaluation, challenges and benefits. *Computers*, *9*(2), 52.
[85]. Mortuza, M. M. G., & Rauf, M. A. (2022). Industry 4.0: An Empirical Analysis of Sustainable Business Performance Model Of Bangladeshi Electronic Organisations. *International Journal of Economy and Innovation*. https://gospodarkainnowacje.pl/index.php/issue_view_32/article/view/826
[86]. Moser, N., Lande, T. S., Toumazou, C., & Georgiou, P. (2016). ISFETs in CMOS and emergent trends in instrumentation: A review. *IEEE Sensors Journal*, *16*(17), 6496-6514.
[87]. Mussard, M., & Amara, M. (2018). Performance of solar photovoltaic modules under arid climatic conditions: A review. *Solar Energy*, *174*, 409-421.
[88]. Naghibi, S. A., Pourghasemi, H. R., & Dixon, B. (2016). GIS-based groundwater potential mapping using boosted regression tree, classification and regression tree, and random forest machine learning models in Iran. *Environmental monitoring and assessment*, *188*(1), 44.
[89]. Ning, D., Yuan, M., Wu, L., Zhang, Y., Guo, X., Zhou, X., Yang, Y., Arkin, A. P., Firestone, M. K., & Zhou, J. (2020). A quantitative framework reveals ecological drivers of grassland microbial community assembly in response to warming. *Nature communications*, *11*(1), 4717.
[90]. Ogbomo, O. O., Amalu, E. H., Ekere, N., & Olagbegi, P. (2017). A review of photovoltaic module technologies for increased performance in tropical climate. *Renewable and sustainable energy reviews*, *75*, 1225-1238.
[91]. Ogbomo, O. O., Amalu, E. H., Ekere, N., & Olagbegi, P. (2018). Effect of operating temperature on degradation of solder joints in crystalline silicon photovoltaic modules for improved reliability in hot climates. *Solar Energy*, *170*, 682-693.
[92]. Otieno, M., Beushausen, H., & Alexander, M. (2016). Chloride-induced corrosion of steel in cracked concrete–Part I: Experimental studies under accelerated and natural marine environments. *Cement and Concrete Research*, *79*, 373-385.
[93]. Palme, M., Inostroza, L., Villacreses, G., Lobato-Cordero, A., & Carrasco, C. (2017). From urban climate to energy consumption. Enhancing building performance simulation by including the urban heat island effect. *Energy and Buildings*, *145*, 107-120.
[94]. Pazos, S. M., Baudino, J. J., Joglar, M. N., Aguirre, F. L., Navarro, C., Palumbo, F., & Silveira, F. (2020). Sensitive Devices and Phase Noise Degradation Mechanisms on all-NMOSFET RF VCO Aging. 2020 Argentine Conference on Electronics (CAE),

[95]. Pham, B. T., Nguyen, M. D., Van Dao, D., Prakash, I., Ly, H.-B., Le, T.-T., Ho, L. S., Nguyen, K. T., Ngo, T. Q., & Hoang, V. (2019). Development of artificial intelligence models for the prediction of Compression Coefficient of soil: An application of Monte Carlo sensitivity analysis. *Science of the total environment*, *679*, 172-184.
[96]. Pushpakaran, B. N., Subburaj, A. S., Bayne, S. B., & Mookken, J. (2016). Impact of silicon carbide semiconductor technology in Photovoltaic Energy System. *Renewable and sustainable energy reviews*, *55*, 971-989.
[97]. Qazi, S. (2016). *Standalone photovoltaic (PV) systems for disaster relief and remote areas*. Elsevier.
[98]. Quansah, D. A., Adaramola, M. S., Appiah, G. K., & Edwin, I. A. (2017). Performance analysis of different grid-connected solar photovoltaic (PV) system technologies with combined capacity of 20 kW located in humid tropical climate. *International Journal of Hydrogen Energy*, *42*(7), 4626-4635.
[99]. Rahmati, O., Pourghasemi, H. R., & Melesse, A. M. (2016). Application of GIS-based data driven random forest and maximum entropy models for groundwater potential mapping: a case study at Mehran Region, Iran. *Catena*, *137*, 360-372.
[100]. Rakibul, H., & Samia, A. (2022). Information System-Based Decision Support Tools: A Systematic Review Of Strategic Applications In Service-Oriented Enterprises. *Review of Applied Science and Technology*, *1*(04), 26-65. https://doi.org/10.63125/w3cevz78
[101]. Rawat, R., Lamba, R., & Kaushik, S. (2017). Thermodynamic study of solar photovoltaic energy conversion: An overview. *Renewable and sustainable energy reviews*, *71*, 630-638.
[102]. Reza, M., Vorobyova, K., & Rauf, M. (2021). The effect of total rewards system on the performance of employees with a moderating effect of psychological empowerment and the mediation of motivation in the leather industry of Bangladesh. *Engineering Letters*, *29*, 1-29.
[103]. Rezaei, E., Donato, M., Patterson, W. R., Zaslavsky, A., & Bahar, R. I. (2020). Fundamental thermal limits on data retention in low-voltage CMOS latches and SRAM. *IEEE Transactions on Device and Materials Reliability*, *20*(3), 488-497.
[104]. Rony, M. A., & Ashraful, I. (2022). Big Data And Engineering Analytics Pipelines For Smart Manufacturing: Enhancing Efficiency, Quality, And Predictive Maintenance. *American Journal of Scholarly Research and Innovation*, *1*(02), 59–85. https://doi.org/10.63125/rze0my79
[105]. Roundy, P. T., Bradshaw, M., & Brockman, B. K. (2018). The emergence of entrepreneurial ecosystems: A complex adaptive systems approach. *Journal of business research*, *86*, 1-10.
[106]. Saikat, S. (2021). Real-Time Fault Detection in Industrial Assets Using Advanced Vibration Dynamics And Stress Analysis Modeling. *American Journal of Interdisciplinary Studies*, *2*(04), 39–68. https://doi.org/10.63125/0h163429
[107]. Saikat, S. (2022). CFD-Based Investigation of Heat Transfer Efficiency In Renewable Energy Systems. *International Journal of Scientific Interdisciplinary Research*, *1*(01), 129–162. https://doi.org/10.63125/ttw40456
[108]. Sampaio, P. G. V., & González, M. O. A. (2017). Photovoltaic solar energy: Conceptual framework. *Renewable and sustainable energy reviews*, *74*, 590-601.
[109]. Sangwan, V. K., & Hersam, M. C. (2020). Neuromorphic nanoelectronic materials. *Nature nanotechnology*, *15*(7), 517-528.
[110]. Schneller, E. J., & Davis, K. O. (2019). Outdoor Field Testing: Environmental and System Stress Factors. In *Durability and Reliability of Polymers and Other Materials in Photovoltaic Modules* (pp. 279-295). Elsevier.
[111]. Shaikh, S., & Aditya, D. (2021). Federated Learning-Driven Predictive Quality Analytics and Supply Chain Optimization In Distributed Manufacturing Networks. *Review of Applied Science and Technology*, *6*(1), 74-107. https://doi.org/10.63125/k18cbz55
[112]. Shaikh, S., & Sudipto, R. (2022). Multi-Objective Thermo-Economic and Supply Chain Optimization Modeling For Hydrogen Energy Integration In Smart Factories. *International Journal of Scientific Interdisciplinary Research*, *1*(01), 163–193. https://doi.org/10.63125/p9y8p705
[113]. Sivula, K., & Van De Krol, R. (2016). Semiconducting materials for photoelectrochemical energy conversion. *Nature Reviews Materials*, *1*(2), 1-16.
[114]. Spinelle, L., Gerboles, M., Villani, M. G., Aleixandre, M., & Bonavitacola, F. (2017). Field calibration of a cluster of low-cost commercially available sensors for air quality monitoring. Part B: NO, CO and CO2. *Sensors and Actuators B: Chemical*, *238*, 706-715.
[115]. Stagni, A., Frassoldati, A., Cuoci, A., Faravelli, T., & Ranzi, E. (2016). Skeletal mechanism reduction through species-targeted sensitivity analysis. *Combustion and Flame*, *163*, 382-393.
[116]. Steinkemper, H., Geisemeyer, I., Schubert, M. C., Warta, W., & Glunz, S. W. (2017). Temperature-dependent modeling of silicon solar cells—Eg, ni, recombination, and VOC. *IEEE Journal of Photovoltaics*, *7*(2), 450-457.
[117]. Surya, S. G., Raval, H. N., Ahmad, R., Sonar, P., Salama, K. N., & Rao, V. R. (2019). Organic field effect transistors (OFETs) in environmental sensing and health monitoring: A review. *TrAC Trends in Analytical Chemistry*, *111*, 27-36.
[118]. Tabor, D. P., Roch, L. M., Saikin, S. K., Kreisbeck, C., Sheberla, D., Montoya, J. H., Dwaraknath, S., Aykol, M., Ortiz, C., & Tribukait, H. (2018). Accelerating the discovery of materials for clean energy in the era of smart automation. *Nature Reviews Materials*, *3*(5), 5-20.
[119]. Taniguchi, S. (2020). Examining the causality structures of electricity interchange and variable renewable energy: a comparison between Japan and Denmark. *Asia-Pacific Journal of Regional Science*, *4*(1), 159-191.
[120]. Täuscher, K., & Laudien, S. M. (2018). Understanding platform business models: A mixed methods study of marketplaces. *European management journal*, *36*(3), 319-329.
[121]. Toledo, C., López-Vicente, R., Abad, J., & Urbina, A. (2020). Thermal performance of PV modules as building elements: Analysis under real operating conditions of different technologies. *Energy and Buildings*, *223*, 110087.

[122]. Tonoy Kanti, C., & Shaikat, B. (2021). Blockchain-Enabled Security Protocols Combined With AI For Securing Next-Generation Internet Of Things (IOT) Networks. *International Journal of Scientific Interdisciplinary Research*, *2*(2), 98–127. https://doi.org/10.63125/pcdqzw41

[123]. Tossa, A. K., Soro, Y., Thiaw, L., Azoumah, Y., Sicot, L., Yamegueu, D., Lishou, C., Coulibaly, Y., & Razongles, G. (2016). Energy performance of different silicon photovoltaic technologies under hot and harsh climate. *Energy*, *103*, 261-270.

[124]. Tress, W., Domanski, K., Carlsen, B., Agarwalla, A., Alharbi, E. A., Graetzel, M., & Hagfeldt, A. (2019). Performance of perovskite solar cells under simulated temperature-illumination real-world operating conditions. *Nature Energy*, *4*(7), 568-574.

[125]. Ulpiani, G., Di Giuseppe, E., Di Perna, C., D'Orazio, M., & Zinzi, M. (2019). Thermal comfort improvement in urban spaces with water spray systems: Field measurements and survey. *Building and Environment*, *156*, 46-61.

[126]. Usman, Z., Tah, J., Abanda, H., & Nche, C. (2020). A critical appraisal of pv-systems' performance. *Buildings*, *10*(11), 192.

[127]. Vu-Bac, N., Lahmer, T., Zhuang, X., Nguyen-Thoi, T., & Rabczuk, T. (2016). A software framework for probabilistic sensitivity analysis for computationally expensive models. *Advances in Engineering Software*, *100*, 19-31.

[128]. Wang, K., Zhang, Q., & Zhang, J. (2019). Evaluation of scale effect of micro electrical discharge machining system. *Journal of Manufacturing Processes*, *38*, 174-178.

[129]. Wang, Y., Banerjee, A., Wehrle, L., Shi, Y., Brandon, N., & Deutschmann, O. (2019). Performance analysis of a reversible solid oxide cell system based on multi-scale hierarchical solid oxide cell modelling. *Energy Conversion and Management*, *196*, 484-496.

[130]. West, B. J., Turalska, M., & Grigolini, P. (2016). Networks of Echoes. *Cham, Switzerland: Springer International Publishing AG*.

[131]. Xiang, C., Zhao, X., Tan, L., Ye, J., Wu, S., Zhang, S., & Sun, L. (2019). A solar tube: Efficiently converting sunlight into electricity and heat. *Nano Energy*, *55*, 269-276.

[132]. Ye, Y., Zhang, W., & Liu, W. (2019). Thermal-aware design and simulation approach for optical NoCs. *IEEE Transactions on Computer-Aided Design of Integrated Circuits and Systems*, *39*(10), 2384-2395.

[133]. Yousif, J. H., Kazem, H. A., & Boland, J. (2017). Predictive models for photovoltaic electricity production in hot weather conditions. *Energies*, *10*(7), 971.

[134]. Zhang, F., Zhao, J., Hu, D., Skoczylas, F., & Shao, J. (2018). Laboratory investigation on physical and mechanical properties of granite after heating and water-cooling treatment. *Rock Mechanics and Rock Engineering*, *51*(3), 677-694.

[135]. Zhang, L., Tan, J., Han, D., & Zhu, H. (2017). From machine learning to deep learning: progress in machine intelligence for rational drug discovery. *Drug discovery today*, *22*(11), 1680-1685.

[136]. Zhang, Y., Ideue, T., Onga, M., Qin, F., Suzuki, R., Zak, A., Tenne, R., Smet, J., & Iwasa, Y. (2019). Enhanced intrinsic photovoltaic effect in tungsten disulfide nanotubes. *Nature*, *570*(7761), 349-353.

[137]. Zobayer, E. (2021a). Data Driven Predictive Maintenance In Petroleum And Power Systems Using Random Forest Regression Model For Reliability Engineering Framework. *Review of Applied Science and Technology*, *6*(1), 108-138. https://doi.org/10.63125/5bjx6963

[138]. Zobayer, E. (2021b). Machine Learning Approaches For Optimization Of Lubricant Performance And Reliability In Complex Mechanical And Manufacturing Systems. *American Journal of Scholarly Research and Innovation*, *1*(01), 61–92. https://doi.org/10.63125/5zvkgg52

[139]. Zuo, X., Li, B., & Yang, J. (2016). Error sensitivity analysis and precision distribution for multi-operation machining processes based on error propagation model. *The International Journal of Advanced Manufacturing Technology*, *86*(1), 269-280.